Strength in Notched and Impact Damaged Laminates

by

Mohamad Samih El-Zein

Dissertation submitted to the Faculty of the

Virginia Polytechnic Institute and State University

in partial fulfillment of the requirements for the degree of

Doctor of Philosophy

in

Engineering Mechanics

APPROVED:

K. L. Reifsnider, Chairman

W. W. Stinchcomb

D. H. Morris

O. H. Griffin

C. W. Smith

August, 1989

Blacksburg, Virginia

Strength in Notched and Impact Damaged Laminates

by

Mohamad Samih El-Zein

K. L. Reifsnider, Chairman

Engineering Mechanics

(ABSTRACT)

The strength of notched and impact damaged laminates was studied. The solution for a plate containing an elliptic opening and inclusion was used as given by Lekhnitskii. The solution for the infinite plate, combined with laminate analysis to determine the ply stresses, and the average stress criterion proposed by Whitney and Nuismer were used to predict the notched strength. However, unlike Whitney and Nuismer, the average stress criterion was used at the ply level.

The strength of off-axis unidirectional laminates was predicted by using a matrix oriented failure criterion applied at a critical point on the boundary of the hole. A good agreement between the experimental and predicted data was obtained. On the other hand, an attempt made to predict the notched strength of angle-ply laminates was not as successful. This is believed to be due to the different failure modes existing among different $[\pm\theta]_s$ laminates.

The controversy on whether the characteristic dimension is a material or geometric property, together with the belief that the physics of fracture of composites is better represented at the ply level, have motivated the author to seek an invariant equation which describes the dependence of the characteristic dimension, D_o . A quantitative approach to determine the characteristic dimension in the average stress criterion was proposed. A good agreement between experimental and predicted data was found. It was also found that contrary to prior claims, the value of D_o does not depend on the diameter

of the hole, when used at the ply level. Moreover, the strength of quasi-isotropic laminates loaded at an angle ϕ with respect to the material x-axis was also studied. Again, excellent agreement between experiment and predictions was shown.

The tensile strength after impact (TSAI) was investigated. An approach based on modeling the delaminated area as an elliptic inclusion was used. The difference between the compliances of the plate and the inclusion was assumed to be proportional to the ratio of the delaminated areas. At low impact energy, a reference area was used. The results obtained using this approach gave good agreement with the experimental data.

Acknowledgements

The work presented in this manuscript was carried out under the direction of professor Kenneth L. Reifsnider and I wish to express great appreciation for his guidence and support throughout this research.

I further wish to express sincere appreciation to Dr. W. W. Stinchcomb , Dr. D. T. Mook, Dr. O. H. Griffin, and Dr. C. W. Smith for serving on my committee and reviewing this manuscript. I would also like to greatly thank my wife who without her love and compassion none of this would have been possible. My appreciation also goes to my mother-in-law for whom I have a lot of love and respect.

Finally, my deepest appreciation goes to my family, who for them I went through all the fun of getting this degree. I wish to dedicate this dissertation to my father and brother ( ) as a mean of expressing my love and appreciation for all the hardships that they lifted me through , and for the patience they had toward me. Thanks also goes to my mom for her love and prayers and to all my friends who made this work possible.

Table of Contents

List of Illustrations

List of Tables

Chapter I

Introduction

The advantages of composite materials in design applications have been well recognized. The presence of notches and impact-damaged zones dramatically affect the performance of composite laminates. In this thesis, both experimental results and predictive analysis for the evaluation of the strength of composite laminates with notches and impact-damaged zones will be presented.

1.1. Notched Strength

In order to represent the complexity of analyzing the fracture behavior of notched composite laminates, several strength models have been proposed. The Waddoups, Eisenmann, and Kaminski [1] model is one of the most widely recognized models employing the use of linear elastic fracture mechanics (LEFM). This model assumes that regions of intense energy, of length 'a' perpendicular to the applied load direction, are developed at the edges of the hole. This model depends on the characteristic length, 'a', and the unnotched strength to predict the notched strength. Moreover, the characteristic length is a function of the material system, ply orientation, and stacking sequence.

It should be noted , however, that the application of LEFM to composite materials is questionable except under very specific conditions as stated by Wu [2]:

1. Flaw orientation with respect to the principal axis of symmetry must be fixed.

2. The definition of stress intensity factors for the anisotropic cases must be analogous to the isotropic case in stress distribution and fracture modes.

3. The critical orientation aligns with one of the principal axes of symmetry.

Furthermore, Whitney and Nuismer [3] also furnished a variety of reasons for the inadequacy of LEFM, two of which are:

1. "single cracks of the types observed in metals do not form in resin matrix composites under repeated loads; and

2. unlike metals , a positive correlation between the unnotched tensile strength of a composite and its fracture toughness seems to exist, the greater the tensile strength the greater the fracture toughness."

In addition to the above, the hole size effect observed in composite materials also makes the concept of the classical stress concentration factor approach inapplicable.

Poe and Sova [4] proposed a fracture model with an approach similar to that of Waddoups et al. Most of the fracture models proposed deal with fiber-dominated laminates exhibiting a linear stress-strain curve up to failure. However, for some configurations a nonlinear stress-strain curve is observed, e.g. for $[\pm 45]_s$ graphite/epoxy laminates. To avoid the problem of nonlinear behavior, Poe and Sova analyzed data based on strains instead of stresses. They proposed a general fracture toughness parameter, Q_c , which is not a function of the laminate orientation. This toughness parameter is determined based on fiber failure in the controlling ply and is proportional to the critical stress intensity factor. A correlation between predictions and experimental data showed good agreement for fiber-controlled fracture. Poe and Sova proposed three different methods for calculating the fracture toughness parameter.

Mar and Lin [5] proposed a fracture model analogous to the classical LEFM equation applied to homogeneous materials. The order of singularity changes from -1/2,

for isotropic material, to an exponent n which is defined as the order of singularity of a crack with its tip at the interface of two different materials, i.e. fiber and matrix. This order of singularity is a property of the materials considered and is a function of the ratio of the shear moduli and the Poisson's ratios of the matrix and the filament. The model also defines a composite fracture toughness H_C, analogous to K_{1C} , however different. This fracture model has two parameters ("n" and "H_C"). The two parameters can be obtained by testing two specimens with two different sizes of discontinuities. Experimental data indicated that the order of singularity, n, is a function of the material stacking sequence. Furthermore, they found that the notched strength is not a function of the type of discontinuity involved.

Whitney and Nuismer [3] proposed two stress criteria for predicting the notched strength. These failure criteria are the point stress criterion and the average stress criterion. Both criteria assume that failure occurs when the stress (at a point or averaged over a distance) ahead of the hole reaches the unnotched tensile strength of the material. These two failure criteria also resort to the use of a characteristic length (d_o for the point stress and a_o for the average stress), however, without the use of the principles of classical LEFM. As in the Waddoups, et. al. , model, the characteristic length depends on the material system, ply orientation, and stacking sequence. It should be noted here that the applicability of these fracture models depends largely on the characteristic dimension which must be known before the notched strength can be predicted. Whitney, et. al. , used a constant value of a_o or d_o to predict the notched strength of composite laminates, and good agreement was found between experiments and predictions. However, several other investigators used these values of the characteristic dimensions, and poor agreement was demonstrated. Hence, the Whitney- Nuismer fracture models would be greatly enhanced if a procedure to obtain the characteristic dimension was formulated, based on the material system and laminate configuration.

Karlak [6] proposed a fracture model by simply modifying the Whitney and Nuismer point stress criterion. Unlike the two previous fracture models, Karlak deduced from test data that the characteristic dimension for the point stress criterion is not a material property, but rather is related to the square root of the hole radius. The principal shortcoming of this model is that it works well in predicting the notched strength of particular laminates but fails for others where it seems that the characteristic distance is independent of the hole radius.

Pipes, Wetherold, and Gillespie [7] also proposed a fracture model based on the Whitney and Nuismer point stress failure criterion. This model can be applied to any multi-directional orthotropic laminate for which the stress concentration factor, K_T, is not equal to 3. Unlike Karlak, Pipes, et. al. , considered a more general exponential relationship between the discontinuity and the characteristic dimension. This fracture model predicts the notched strength of the laminate provided that the laminate unnotched strength (σ_o), the exponential parameter (m), and the notch sensitivity factor (C) are known. These parameters depend on many factors such as the fiber-matrix and matrix-matrix interfacial bonding, the fiber orientation and laminate configuration, and the constituent properties. Moreover, the values of σ_o , m, and C affect the stress concentration factor. The parameters are determined experimentally by one unnotched specimen and two notched specimens having two different hole radii. Simply, the Pipes et al fracture model is empirical, with three parameters. Like the other fracture models, an agreement between experiment and prediction was found for the cases tested.

For more detailed theoretical background related to the theories discussed above, the reader is referred to the review paper by Awerbuch and Madhukar [8]. In summary, many failure criteria have been proposed. However, most of these require a characteristic dimension and the laminate strength to be known, a priori, and none are soundly enough based on fundemental principles to be universally applicable or generally accepted.

1.2. Residual Strength After Impact

Due to their high strength-to-weight and stiffness-to-weight ratios, composites (as mentioned earlier) have received a great deal of attention and have been employed in many design applications, especially in aeronautical structures. These highly stressed structures make the behavior of composite materials under impact conditions a problem that deserves close attention. Events such as a tool drop and vehicular impact are simple examples of impact on aircraft structures.

Unlike metals, composites suffer a severe reduction in their residual strength after impact. The damage induced as a result of impact plays the role of a stress raiser in the material when loaded. Consequently, the philosophy of modelling impact damage as an implanted hole [9-11] evolved. Husman, et.al., [10] presented a model for predicting the residual strength after impact (RSAI) as a function of the kinetic energy of impact. It was shown that for velocities below the penetration velocity , the predictions gave good correlations with the experimental data. The damaged area was represented as an equivalent flaw of well defined size and shape, artificially introduced into the material. Caprino [9], proposed a model to predict the RSAI based on a fracture mechanics approach used by Mar and Lin [5] to evaluate the notched strength of a laminate. Similar to Husman, et. al., Caprino's formulation was a function of the kinetic energy of impact. Moreover, Caprino defined a characteristic defect on the premise that the laminate strength is not influenced by flaws smaller than the characteristic flaw. Furthermore, Avva and Padmanabha [11] used the average stress criterion concept, introduced by Whitney and Nuismer [3], to predict the RSAI. The impact damage was modelled as an implanted hole, and an expression in terms of the kinetic energy and a characteristic dimension was derived.

The models proposed by [9-11] gave good correlation with experimental results. However, from a practical point of view, the impact energy is an unknown. Therefore, a prediction based on measurable quantities is needed. The following analysis introduces a model to predict the RSAI as a function of the delaminated area caused by impact damage. This damaged zone is simulated as an elliptical inclusion. The prediction is carried out using the solution of an infinite plate containing an elliptical inclusion given by Lekhnitskii [12], and an average stress criterion is applied at the controlling-ply level.

1.3. Problem Definition and Research Objectives

The fracture model of Whitney, et. al., discussed in section 1.1 seems to yield good results in predicting the notched strength of composite laminates, when the characteristic dimension is known. However, there is a controversy on whether the characteristic dimension is a material property or a geometric one. Some researchers have used the characteristic dimension as a constant for the same material system, others proposed that it is a function of the geometry, and some reached the conclusion that the characteristic parameter is a function of material properties, stacking sequence, and other factors.

The above controversy, together with the belief that the physics of fracture of composites is better represented at the ply level, have motivated some of the work presented here. A systematic methodology to determine the characteristic dimension and predict the notched strength of composite laminates will be presented. Moreover, this concept will be extended to predict the residual strength in a plate with an elastic inclusion. This inclusion will be the result of impact -induced damage, and can vary from an open hole to a rigid core.

In chapter 2, the theoretical background of the problem of elliptical inclusion and open hole will be presented. This will be followed by the results of an experimental and theoretical investigation of notched strength in chapter 3. In the next chapter, 4, a model for predicting the tensile strength after impact will be proposed. Both experimental and predicted data will be presented. Finally, in chapter 5, conclusions relevant to the results acquired will be drawn.

Chapter II

Theoretical Analysis

It is well known that the presence of a discontinuity in a material component reduces the strength and produces stress concentrations around the boundary of the discontinuity. The presence of a circular opening in a plate produces a stress concentration with a factor of 3 for isotropic material, or higher (or lower) depending on the degree of anisotropy of the material.

Solutions to the problems of the determination of stresses in an anisotropic plate weakened by an elliptical opening and a plate containing an elliptical inclusion were derived by Lekhnitskii [12]. The solutions are in terms of complex potentials and will be reproduced here to clarify limitations and the nomenclature adopted. A simple review of plane anisotropic elasticity will also be presented.

2.1. Anisotropic Elasticity

The two-dimensional solution to both the open hole and the elastic inclusion is one of the generalized plane stress type , i.e., the in-plane stresses are averaged through the thickness as follows

$$\bar{\sigma}_x = \int_{-h/2}^{h/2} \sigma_x \, dz$$

$$\bar{\sigma}_y = \int_{-h/2}^{h/2} \sigma_y \, dz \qquad [2.1.1]$$

$$\bar{\tau}_{xy} = \int_{-h/2}^{h/2} \tau_{xy}\, dz$$

where h is the thickness of the laminate, z is the through-the-thickness coordinate, and the overbar stands for an average quantity. The overbar will be dropped with the understanding that the stresses are averaged through the thickness. The remainder of the stress components are negligible. The in-plane strains are determined from the two displacements u and v using the following kinematic assumptions

$$\varepsilon_x = \frac{\partial u}{\partial x}$$

$$\varepsilon_y = \frac{\partial v}{\partial y} \qquad [2.1.2]$$

$$\gamma_{xy} = \frac{\partial v}{\partial x} + \frac{\partial u}{\partial y}$$

Therefore, the average in-plane stresses can be related to the average in-plane strains using Hooke's law, or, in terms of compliance, the strains can be related to the stresses as

$$\begin{Bmatrix} \varepsilon_x \\ \varepsilon_y \\ \gamma_{xy} \end{Bmatrix} = \begin{bmatrix} a_{11} & a_{12} & a_{16} \\ a_{12} & a_{22} & a_{26} \\ a_{16} & a_{26} & a_{66} \end{bmatrix} \begin{Bmatrix} \sigma_x \\ \sigma_y \\ \tau_{xy} \end{Bmatrix} \qquad [2.1.3]$$

where a_{ij} are the elements of the engineering compliance matrix.

The equations of equilibrium for the plane problem can be written in terms of the average stresses as

$$\frac{\partial \sigma_x}{\partial x} + \frac{\partial \tau_{xy}}{\partial y} + X = 0$$

[2.1.4]

$$\frac{\partial \tau_{xy}}{\partial x} + \frac{\partial \sigma_y}{\partial y} + Y = 0$$

where X and Y are the body forces.

At this point a stress function F is defined such that

$$\sigma_x = \frac{\partial^2 F}{\partial y^2} + \Psi$$

$$\sigma_y = \frac{\partial^2 F}{\partial x^2} + \Psi \qquad [2.1.5]$$

$$\tau_{xy} = -\frac{\partial^2 F}{\partial x \, \partial y}$$

where Ψ is the body force potential defined as

$$X = -\frac{\partial \Psi}{\partial x}$$

and

$$Y = -\frac{\partial \Psi}{\partial y}$$

To insure single-valued continuous strain field, and since the problem is a plane one, the strains are not independent but are related by the following compatibility equation

$$\frac{\partial^2 \varepsilon_x}{\partial y^2} + \frac{\partial^2 \varepsilon_y}{\partial x^2} = \frac{\partial^2 \gamma_{xy}}{\partial x \, \partial y} \qquad [2.1.6]$$

The other five compatibility equations are identically satsified. Substituting the stress function , F, defined in equation [2.1.5] and equation [2.1.3] into equation [2.1.6] will yield the following fourth order homogeneous differential equation

$$a_{22} \frac{\partial^4 F}{\partial x^4} - 2a_{26} \frac{\partial^4 F}{\partial x^3 \, \partial y} + (2a_{12} + a_{66}) \frac{\partial^4 F}{\partial x^2 \, \partial y^2} - 2a_{16} \frac{\partial^4 F}{\partial x \partial y^3} \qquad [2.1.7]$$

$$+ a_{11} \frac{\partial^4 F}{\partial y^4} = 0$$

where the body forces have been neglected. It should be noted that equation [2.1.7] reduces to the well-known biharmonic equation if the material is isotropic, i.e. $a_{16} = a_{26} = 0, \quad a_{12} = -\frac{v}{E}, \quad a_{66} = \frac{1}{G}, \quad$ and $G = \frac{E}{[2(1+v)]}$.
Equation (2.1.7) can be rewritten in a compacted form as

$$D_1 \, D_2 \, D_3 \, D_4 \, F = 0 \qquad [2.1.8]$$

where the operators D_i are defined as:

$$D_i = \left[\frac{\partial}{\partial y} - \mu_i \frac{\partial}{\partial x} \right] \qquad (i = 1,2,3,4) \qquad [2.1.9]$$

and μ_i are the roots of the following characteristic equation

$$a_{11}\mu^4 - 2a_{16}\mu^3 + [2a_{12} + a_{66}]\mu^2 - 2a_{26}\mu + a_{22} = 0 \qquad [2.1.10]$$

It was shown by [12] that the roots of equation [2.1.10] are either complex or pure imaginary. Hence, a pair of complex conjugate roots are obtained

$$\mu_1 = \alpha + \beta i$$

$$\mu_2 = \gamma + \delta i$$

$$\bar{\mu}_1 = \alpha - \beta i \qquad [2.1.11]$$

$$\bar{\mu}_2 = \gamma - \delta i$$

To simplify the analysis, a set of new coordinates is introduced

$$z_1 = x + \mu_1 y$$

$$z_2 = x + \mu_2 y$$

$$\bar{z}_1 = x + \bar{\mu}_1 y \qquad [2.1.12]$$

$$\bar{z}_2 = x + \bar{\mu}_2 y$$

Due to the fact that the stresses should be real and the coefficients in equation [2.1.7] are constant, the stress function, F, can be written as

$$F = 2\,\mathrm{Re}[F_1(z_1) + F_2(z_2)] \qquad [2.1.13]$$

Furthermore, for further simplification, two new functions are introduced , $\Phi_1(z_1)$ and $\Phi_2(z_2)$ such that

$$\Phi_1(z_1) = \frac{dF_1}{dz_1} \qquad [2.1.14]$$

$$\Phi_2(z_2) = \frac{dF_2}{dz_2}$$

Therefore, using equations [2.1.12], [2.1.13], and [2.1.14] the stresses can be written in terms of the new functions as

$$\sigma_x = 2\,\mathrm{Re}\left[\mu_1^2\,\Phi'_1(z_1) + \mu_2^2\Phi'_2(z_2)\right]$$

$$\sigma_y = 2\,\mathrm{Re}\left[\,\Phi'_1(z_1) + \Phi'_2(z_2)\right] \qquad [2.1.15]$$

$$\tau_{xy} = -\,2\,\mathrm{Re}\left[\mu_1\,\Phi'_1(z_1) + \mu_2\Phi'_2(z_2)\right]$$

and the equations for the in-plane displacements are given by

$$u = 2\,\mathrm{Re}\left[p_1\Phi_1(z_1) + p_2\Phi_2(z_2)\right] - \omega y + u_o$$

$$v = 2\,\mathrm{Re}\left[q_1\Phi_1(z_1) + q_2\Phi_2(z_2)\right] - \omega x + v_o \qquad [2.1.16]$$

where ω, u_o, and v_o are arbitrary constants which characterize the rigid body rotation and the translational displacement, respectively, and

$$p_l = a_{11}\mu_l^2 + a_{12} - a_{16}\mu_l \qquad [2.1.17]$$

$$q_i = a_{12}\mu_l + \frac{a_{22}}{\mu_l} - a_{26}, \qquad (i = 1,2)$$

The normal and tangential stresses along the boundary are found using the following transformation

$$\sigma_n = \sigma_x \cos^2(n,x) + \sigma_y \cos^2(n,y) + 2\tau_{xy} \cos(n,x) \cos(n,y)$$

$$\tau_n = (\sigma_y - \sigma_x)\ \cos(n,x) \cos(n,y) + \tau_{xy}\left[\,\cos^2(n,x) - \cos^2(n,y)\right] \qquad [2.1.18]$$

where n is the normal to the boundary.

The above define the equations necessary for solving problems in plane anisotropic elasticity.

2.2. Anisotropic Plate Containing an Elliptical Opening

The solution for determining the stresses in an anisotropic plate containing an elliptical opening and pulled by a force p at an angle ϕ in relation to the major axis of the ellipse, as shown in figure 1, was obtained by Lekhnitskii [12]. As shown in section 2.1, the problem reduces to finding two functions Φ_1 and Φ_2. These functions are simply presented here as derived in [12]

$$\Phi_1(z_1) = \frac{\overline{\beta}_1 - \mu_2\overline{\alpha}_1}{(\mu_1 - \mu_2)\,\zeta_1}, \quad \Phi_2(z_2) = -\frac{\overline{\beta}_1 - \mu_1\overline{\alpha}_1}{(\mu_1 - \mu_2)\,\zeta_2} \qquad [2.2.1]$$

where

$$\overline{\alpha}_1 = -\frac{p \sin\phi}{2}(a \sin\phi - ib \cos\phi)$$

$$\overline{\beta}_1 = \frac{p \cos\phi}{2}(a \sin\phi - ib \cos\phi) \qquad [2.2.2]$$

$$\zeta_i = \frac{z_i + \sqrt{z_i^2 - a^2 - \mu_i^2 b^2}}{a - i\mu_i b} \quad (i = 1, 2)$$

and a and b are the major and minor axes respectively.

The components of stress can be found by adding the stresses in a plate subjected to uniform stress, i.e.

$$\sigma_x^o = p\,\cos^2\phi, \quad \sigma_y^o = p\,\sin^2\phi, \quad \tau_{xy}^o = p\,\sin\phi\cos\phi \qquad [2.2.3]$$

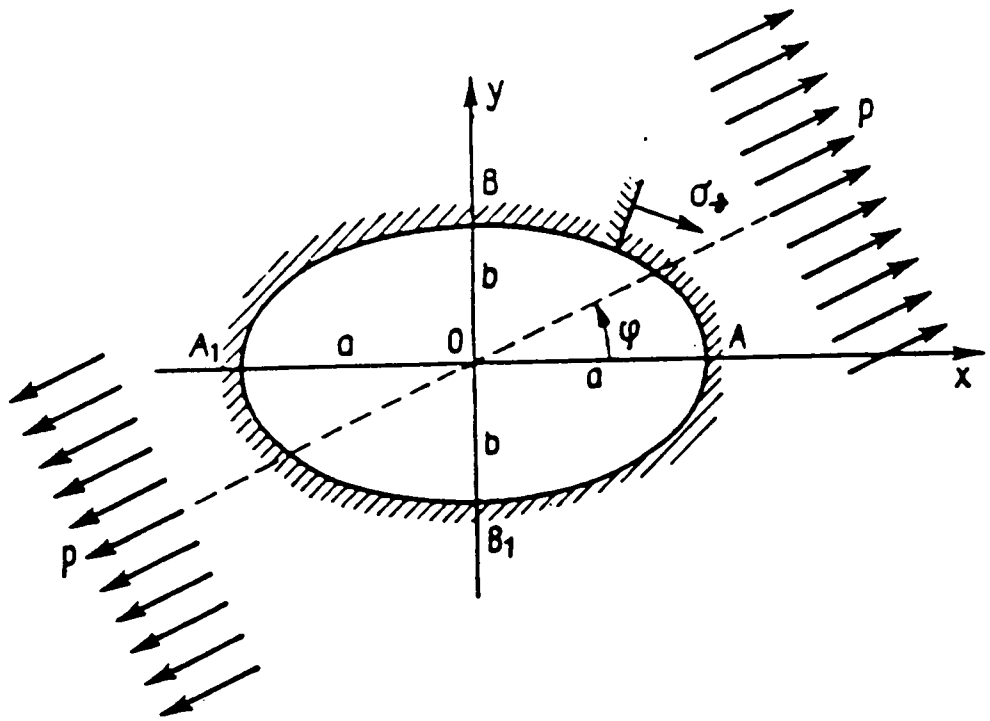

Figure 1. An infinite anisotropic plate containing an elliptic opening subjected to a tensile load at an angle ϕ.

to those obtained from the functions $\Phi_1(z_1)$ and $\Phi_2(z_2)$defined in equation (2.2.1). An important formula which will be used later on is the stress at the diametral ends of the ellipse perpendicular to the applied load when $\phi = 0$. The stress value at points B and B_1 as shown in figure 1 is given by

$$\sigma = P\left[1 + \frac{\beta + \delta}{c}\right] \qquad [2.2.4]$$

where β and δ are the imaginary parts of the roots μ_1 and μ_2 and $c = \frac{a}{b}$.
From equation [2.2.4] it is seen that the ratio $\frac{\beta + \delta}{c}$ defines the stress concentration factor at points B and B_1 and controls the stress distribution away from the hole. This will be used to determine the characteristic dimension D_o in the average stress criterion. It should be noted that for values of ϕ different from zero, The maximum stresses do not occur at points B and B_1. Therefore, a correction relative to the point where the average stress criterion should be applied is needed. This is accompished by scanning the hole for the location of maximum stress and then applying the failure criterion at that point.

2.3. Anisotropic Plate with an Elliptical Inclusion

Using the results obtained for the plate with an elliptic opening, it is possible to solve a more general problem; an anisotropic plate with a bonded or glued center made of an elastic or rigid material.

Consider a plate with an elliptic inclusion subjected to tensile and shear forces uniformly distributed on its sides as shown in figure 2. A stress function can be written in terms of these stresses such that

$$F^o = \frac{1}{2} qx^2 - txy + \frac{1}{2} py^2 \qquad [2.3.1]$$

where p and q are the tensile stresses in the x and y directions respectively and t is the shear stress. The conditions at the points of contact on the surface of the inclusion and the plate are given by

$$X_n = -X'_n, \quad Y_n = -Y'_n \qquad [2.3.2]$$

$$u = u', \quad v = v'$$

These conditions are illustrated in figure 3. X_n and Y_n are forces per unit area acting at the inclusion edge and (') stands for inclusion properties.

After some transformation, the conditions in equation [2.3.2] become

$$2\,Re\,[\Phi_1(z_1) + \Phi_2(z_2)] = \frac{\partial(F' - F^o)}{\partial x} + C_1$$

$$2\,Re\,[\mu_1\Phi_1 + \mu_2\Phi_2] = \frac{\partial(F' - F^o)}{\partial y} + C_2$$

$$2\,Re\,[p_1\Phi_1 + p_2\Phi_2] = u' - u_o + \omega y - u^o \qquad [2.3.3]$$

$$2\,Re\,[q_1\Phi_1 + q_2\Phi_2] = v' - v_o - \omega x - v^o$$

where C_1, C_2, ω, u_o, and v_o are determined from simple additional boundary conditions that depend on the plate shape and the distribution of forces. The stress function F' is the result of the constant stresses in the inclusion, and is given by

$$F' = \frac{1}{2} Bx^2 - Cxy + \frac{1}{2} Ay^2 \qquad [2.3.4]$$

and the constants A, B, and C are defined as

$$\sigma'_x = A, \quad \sigma'_y = B, \quad \tau'_{xy} = C \qquad [2.3.5]$$

The additional stresses in the plate which introduce the effect of the inclusion are given by the functions Φ_1 and Φ_2 as given in [11] :

$$\Phi_1(z_1) = \frac{1}{2(\mu_1 - \mu_2)} [(A-p)bi - (B-q)\mu_2 a + (C-t)(i\mu_2 b - a)] \frac{1}{\zeta_1}$$

$$\Phi_2(z_2) = \frac{1}{2(\mu_1 - \mu_2)} [(A-p)bi - (B-q)\mu_1 a + (C-t)(i\mu_1 b - a)] \frac{1}{\zeta_2} \qquad [2.3.6]$$

where A, B, and C are the stresses in the inclusion and are determined by substituting Φ_1, Φ_2, F^o, and F' in equation [2.3.3]. This results in a set of four equations, two of which are :

$$\left[\frac{p_1 - p_2}{\mu_1 - \mu_2} ib - a'_{11} a \right] A + \left[\frac{\mu_1 p_2 - \mu_2 p_1}{\mu_1 - \mu_2} - a'_{12} \right] aB$$

$$- \left[\frac{(p_1 - p_2)a + i(\mu_1 p_2 - \mu_2 p_1)b}{\mu_1 - \mu_2} + a'_{16} a \right] C + ib(\omega' - \omega)$$

$$= \left[\frac{p_1 - p_2}{\mu_1 - \mu_2} ib - a_{11} a \right] p + \left[\frac{\mu_1 p_2 - \mu_2 p_1}{\mu_1 - \mu_2} - a_{12} \right] qa$$

$$- \left[\frac{(p_1 - p_2)a + i(\mu_1 p_2 - \mu_2 p_1)b}{\mu_1 - \mu_2} + a_{16} a \right] t$$

$$\left[\frac{q_1 - q_2}{\mu_1 - \mu_2} ib - ia'_{12} b - a'_{16} a \right] A + \left[\frac{\mu_1 q_2 - \mu_2 q_1}{\mu_1 - \mu_2} a - ia'_{22} b - a'_{26} a \right] B \qquad [2.3.7]$$

$$-\left[\frac{(q_1-q_2)a+i(\mu_1 q_2-\mu_2 q_1)b}{\mu_1-\mu_2}+a'_{66}a+ia'_{26}b\right]C-a(\omega'-\omega)$$

$$=\left[\frac{q_1-q_2}{\mu_1-\mu_2}ib-ia_{12}b-a_{16}a\right]p+\left[\frac{\mu_1 q_2-\mu_2 q_1}{\mu_1-\mu_2}a-ia_{22}b-a_{26}a\right]q-$$

$$\left[\frac{(q_1-q_2)a+i(\mu_1 q_2-\mu_2 q_1)b}{\mu_1-\mu_2}+a_{66}a+ia_{26}b\right]t$$

the remaining two equations are determined from the above by replacing i by -i and taking the complex conjugates of p_1, p_2, q_1, q_2, μ_1, and μ_2 .

It should be noted that all the other quantities are as defined in section 2.2. Therefore, upon finding A, B, and C the stresses in the plate can be found.

The a'_{ij} used in equation [2.3.7] are the elements of the compliance matrix of the inclusion. These elements can be related to the compliance elements of the plate by a simple linear relationship as follows

$$a'_{ij}=m\,a_{ij} \qquad [2.3.8]$$

In the case of rigid inclusion m is equal to zero , and in the case of open hole m is equal to infinity.

2.4. Failure Criterion

The average stress criterion proposed by Whitney and Nuismer [3] is used to predict the strength. The average stress criterion considers failure to occur when the average stress over a distance D_o reaches the unnotched strength of the laminate. In mathematical form it is written as

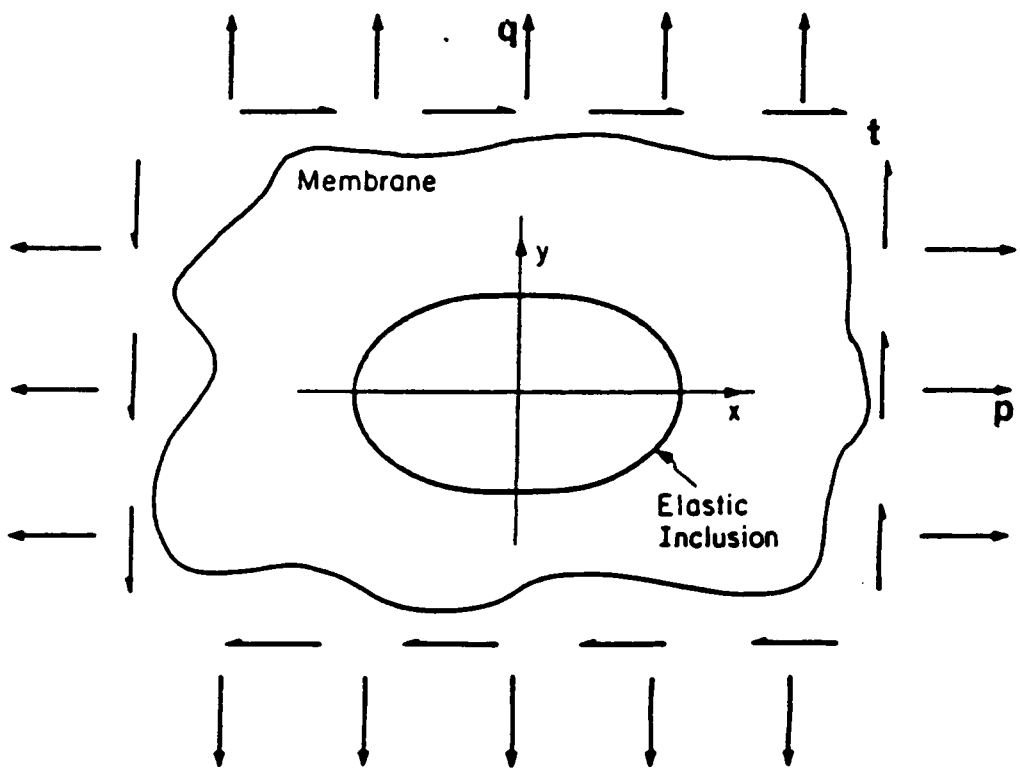

Figure 2. An infinite anisotropic plate containing an elliptic inclusion subjected to uniform loading conditions.

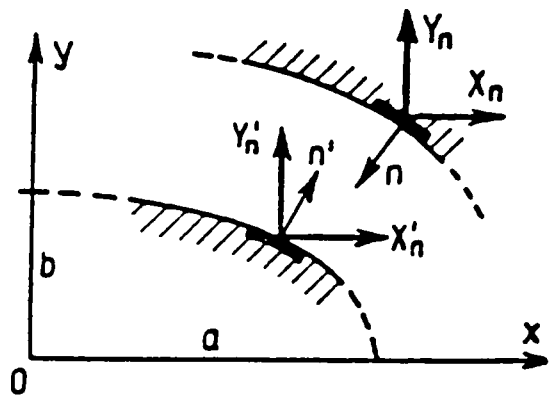

Figure 3. Illustrations of the conditions on the contact surface of the inclusion and the plate.

$$\frac{1}{D_O}\int_{b}^{b+D_O}\sigma_x(0,y)\,dy = \sigma_o \qquad [2.4.1]$$

where σ_o is the unnotched strength of the laminate and σ_y is the global stress in the y-direction.

In this research, the average stress criterion is used, however, with some modification. Instead of using the laminate unnotched strength , the average stress is calculated at the controlling ply level. The failure criterion becomes

$$\frac{1}{D_O}\int_{b}^{b+D_O}\frac{\sigma_1(0,y)}{X_T}\,dy = 1 \qquad [2.4.2]$$

where σ_1 is the stress in the principal direction and X_T is the tensile strength of the material at the ply level. The left hand side of equation [2.4.2] will be referred to as the failure function and will be denoted by F.

Chapter III

Strength Prediction of Composite Laminates Containing a Circular Hole

The notched strength of composite laminates containing circular holes or straight cracks has been the subject of study for the past 20 years. Most of the work on this topic has been devoted to fiber dominated laminates, where it was believed that the characteristic dimension is a constant, as discussed in chapter I. In this chapter, Fiber dominated laminates are also studied, and it is shown that the charateristic dimension is not a constant, but rather is a function of the stacking sequence and the material unidirectional properties. An attempt was also made to characterize and predict the strength of unidirectional off-axis and angle ply laminates. For the off-axis unidirectional laminates, good agreement between experimental and predicted strength was found. This agreement is believed to be dependent upon the occurence of identical failure modes (i.e. shear failure). On the other hand, for the $[\pm\theta]$ angle-ply laminates, accurate strength predictions were not achieved due to the different failure modes associated with different configurations. The notched strength of $[0/\pm\theta]_s$ laminates was also studied. A good agreement was found between the predictions and the experimental data. A method for finding the characteristic dimension based on the material properties was proposed. Finally, the strength of quasi-isotropic laminates loaded at an angle to the material axis was investigated. A detailed discussion and analysis will be presented in the following sections.

3.1. Prediction Procedure

The theory for the field stresses of a plate containing an elliptic opening was presented in chapter II. The strength of the notched composite plate is predicted using an average fiber stress criterion in the ply that controls final failure. This failure criterion assumes failure to occur when the average stress, in a controlling ply, over a distance D_o ahead of the hole boundary reaches the unidirectional tensile strength of the material (equation [2.4.2]).

A computer program was developed in order to compute and integrate the stresses. The procedure followed is outlined in figure 4. The field stresses are determined from the Lekhnitskii solution and, using laminate analysis, the point-wise in-plane force resultants are obtained using

$$\{N\} = \{\sigma_G\}\, H \qquad [3.1.1]$$

where σ_G = global stresses and H = thickness of the laminate.
The laminate strains are found using the in-plane load as

$$\{\varepsilon\} = [A]^{-1}\, \{N\} \qquad [3.1.2]$$

where [A] is the extensional stiffness matrix. Hence, the ply stresses are determined using the reduced stiffness matrix for each ply by

$$\{\sigma_P\} = [\overline{Q}]\{\varepsilon\} \qquad [3.1.3]$$

where σ_P are the ply stresses. The ply stresses are then substituted into equation [2.4.2] to determine the value of the failure function, F.

It is important to note that the average stress criterion is applied at the ply level, rather than at the laminate level as suggested by Whitney and Nuismer [3]. Thus, the influence of ply orientations enters the ply stress calculation, and it is reasonable to ex-

GLOBAL STRESSES OBTAINED FROM

LEKHNITSKII'S SOLUTION

PLY STRESSES USING LAMINATE

ANALYSIS

FAILURE CRITERION APPLIED ON

THE PLY LEVEL

EVALUATION OF THE STRENGTH

Figure 4. The theoretical procedure for predicting the notched strength.

pect that all laminates of a given material can be described with a single set of material parameters. Moreover, the physics of failure of fiber composite laminates is better represented at the ply level. It is important to note that the direction over which the stresses are integrated is the direction which will result in the maximum value for the failure function, F (i.e. F = 1).

3.2. Experiment, Prediction, and Discussion

The experimental program was carried out using an MTS testing machine with 100,000 lb. load capacity. At least five specimens were tested for each stacking sequence.

Specimen Fabrication:

The specimens were made up of AS4/3502 graphite/epoxy, the unidirectional properties of which are given in table 1. The manufacturing process and the cure cycle were as proposed by the manufacturer. Curing was accomplished using an autoclave. The laminates were cured so as to have 65% fiber volume fraction. The laminates were checked for voids or cure defects using an ultrasonic C-scan procedure. A typical C-scan is shown in figure 5. The coupon specimens were then cut using a diamond blade, and the center holes were drilled by means of a carbide drilling bit. The overall dimensions are shown in figure 6.

Unidirectional Off-Axis Laminates:

For unnotched composite laminates, the analysis and predictions of failure have been extensively considered. However for notched off-axis composite laminates, no attempt has been made, to the author's knowledge , to predict the strength. Intuitively,

Table 1.

The unidirectional properties of AS4/3502 Graphite/Epoxy.

E_1 (MSI)	E_2 (MSI)	ν_{12}	G_{12} (MSI)
20.5	1.47	0.30	0.84

X_T (KSI)	X_C (KSI)	Y_T (KSI)	Y_C (KSI)	S_{12} (KSI)
246	200	10.5	64	15

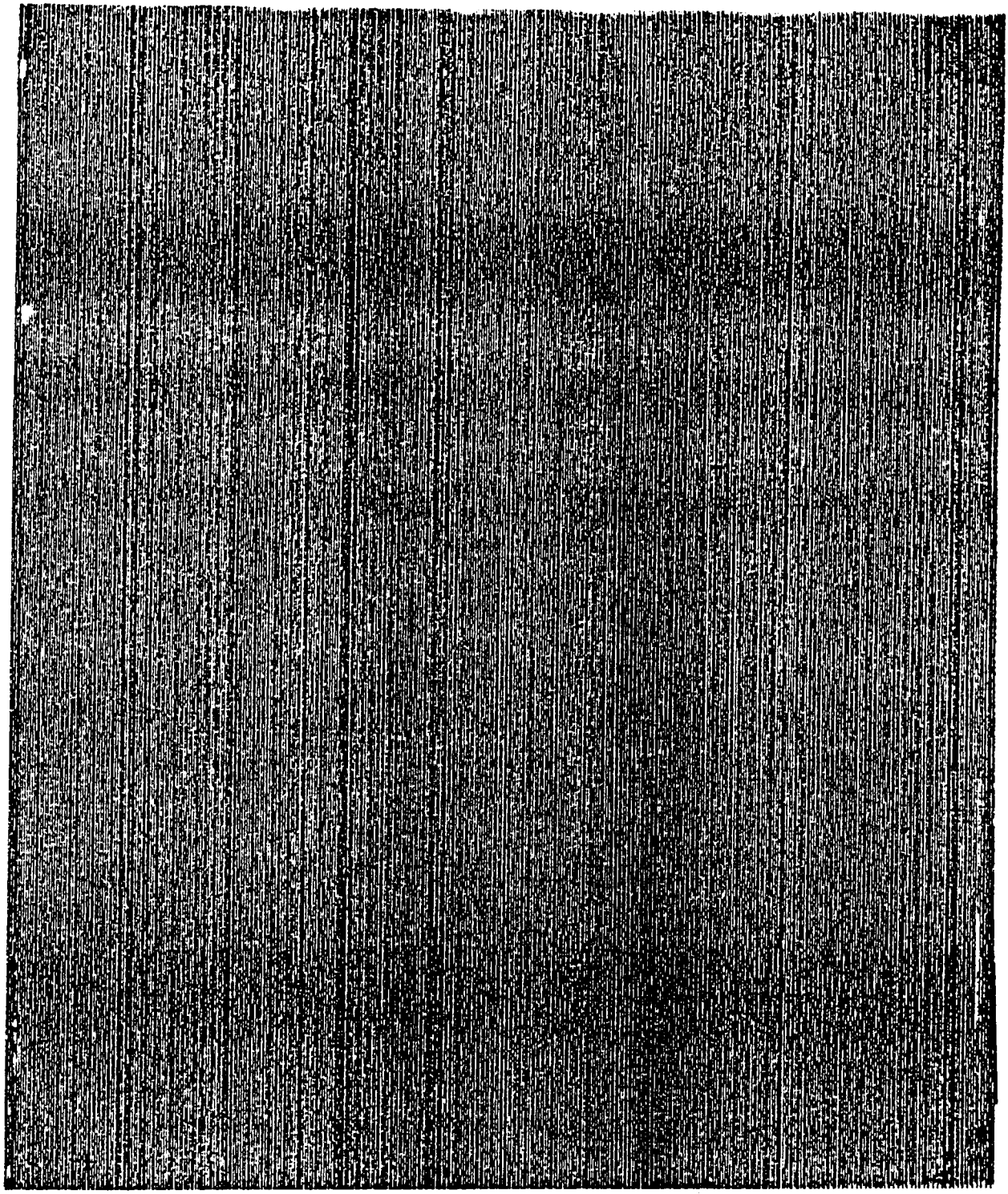

Figure 5. A typical ultrsonic C-scan of AS4/3502 laminate.

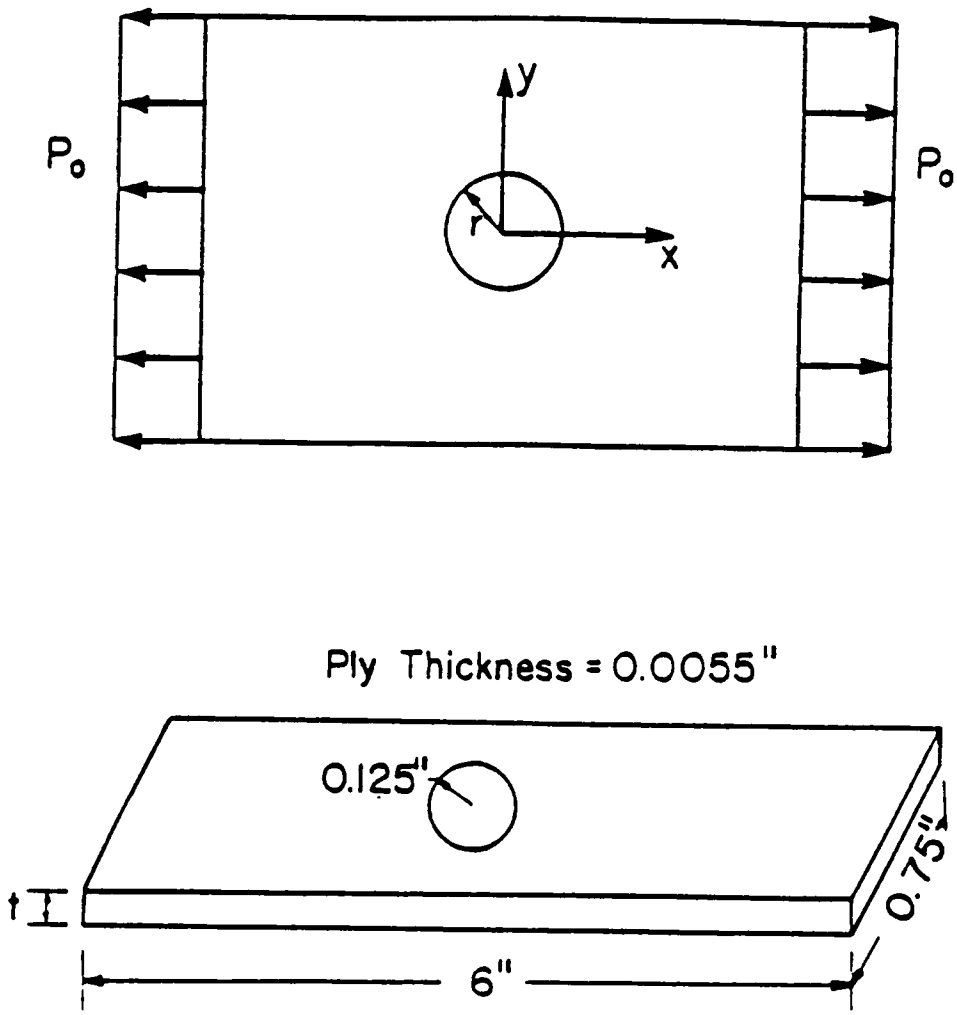

Figure 6. The experimental specimen used in determining the notched strength.

one expects notched off-axis unidirectional laminates to fail in shear. Indeed, experimentally and analytically this has been the case. Figure 7 exhibits the failure of the off-axis unidirectional laminates. Figure 8 demonstrates that failure initiates at the hole boundary and propagates in the direction parallel to the fibers, leading to total separation. It is believed that a critical state of stress exists at the edge of the hole perpendicular to the load direction, which controls the failure initiation in the specimen. Hence, a matrix failure criterion was applied at the critical point to obtain the predicted strength of the laminate. Mathematically, this could be represented as

$$\left[\frac{\sigma_2(0,r)}{Y}\right]^2 + \left[\frac{\sigma_{12}(0,r)}{S}\right]^2 = 1 \qquad [3.2.1]$$

where σ_2 and σ_{12} are the transverse tensile stress and the shear stress in the principal direction respectively, and S and Y are the strength in shear and transverse tension.

The experimental and predicted strength of the off-axis unidirectional laminates are listed in table 2. It is apparent that good agreement between the experimental and predicted data exist. It should be noted that equation [3.2.1] is a point stress criterion with the characteristic dimension equal to zero.

Angle-Ply Laminates:

Five angle ply configurations were selected for testing: $[0]_8$, $[\pm 10]_{2S}$, $[\pm 25]_{2S}$, $[\pm 35]_{2S}$, and $[\pm 45]_{2S}$. Experimentally, consistent data were obtained for each laminate. Nevertheless, attempts to predict the strength were not entirely successful. This is attributed to the different failure modes existing among these configurations.

The failure of the $[\pm 10]_{2S}$ laminate was characterized by fiber pullout and fiber breakage. Similar characteristics were observed for the $[\pm 25]_{2S}$ laminate with less fiber breakage. On the other hand, the failure of the $[\pm 35]_{2S}$ and $[\pm 45]_{2S}$ laminate was

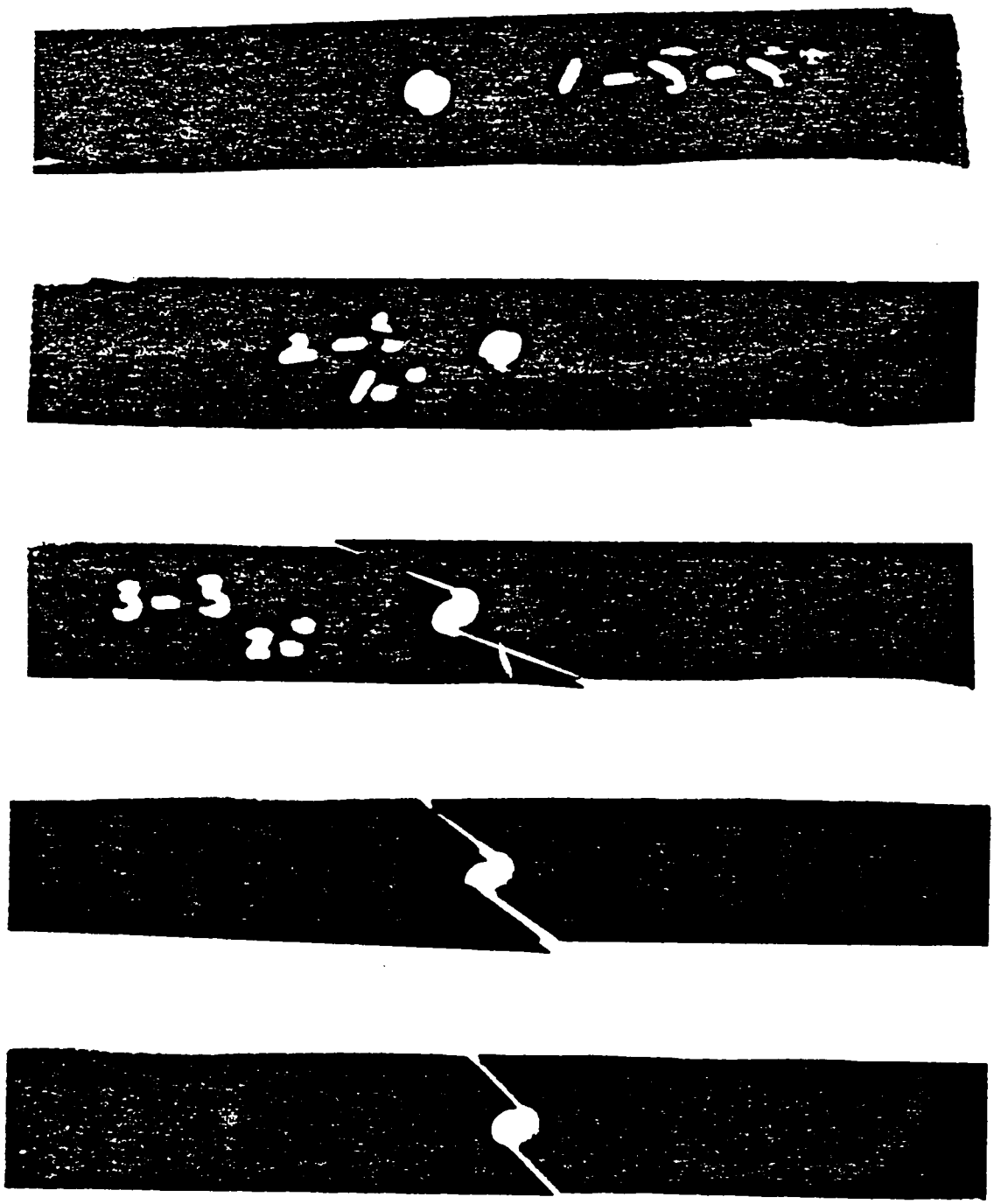

Figure 7. The failure mode of the unidirectional off-axis laminates.

Table 2.

The experimental and predicted strength of the off-axis unidirectional $[\theta]_8$ laminates.

θ	P_{EX}	P_{PR}
5	26.9	27.5
10	16.4	15.7
20	12.4	10.4
35	8.1	7.70
45	5.9	6.55

typified by more shear failure and less fiber breakage. Similar observations were reported by Ginty and Chamis [12].

Because of those different failure properties, a single practical failure criterion which could predict the strength of such laminates was not achieved. The experimental data acquired are shown in figure 8, where the normalized stresses are plotted versus the angle of orientation.

$[0/\pm\theta]_S$ Laminates:

For the case of $[0/\pm\theta]_S$, six configurations were tested: $[0/\pm 10]_S$, $[0/\pm 25]_S$, $[0/\pm 35]_S$, $[0/\pm 45]_S$, $[0/\pm 65]_S$, and $[0/90_2]_S$. The presence of the 0^o ply governs the failure of such laminates. Hence, the failure of the laminate is characterized by the failure of the 0^o ply. The procedure described previously for the computation of stresses and for integrating those stresses according to equation [2.3.2] is followed here for the 0^o ply.

In the first attempt to predict the strength, computation was started by computing a D_o from one of the configurations, and then using that D_o value as a basis to predict the strength of the other laminates. This method is usually used to predict the strength of fiber dominated materials. This procedure yielded poor predictions of the strength of the laminates, which motivated the author to seek another alternative.

It is well known that the stresses on the boundary of the holes of such configurations generally reach a maximum and then reduce sharply until they reach essentially the applied stress value. Because an average of the stresses over a distance D_o will determine the failure load, it was essential to use the stress distribution to find D_o for each configuration. The normalized stresses in the 0^o ply versus the distance away from the hole are plotted for each laminate configuration in figure 9. Analytically, failure of all laminates occured at approximately the same ratio of $\frac{\sigma_1(o,y)}{X_T} = 0.65$ as shown in figure 9.

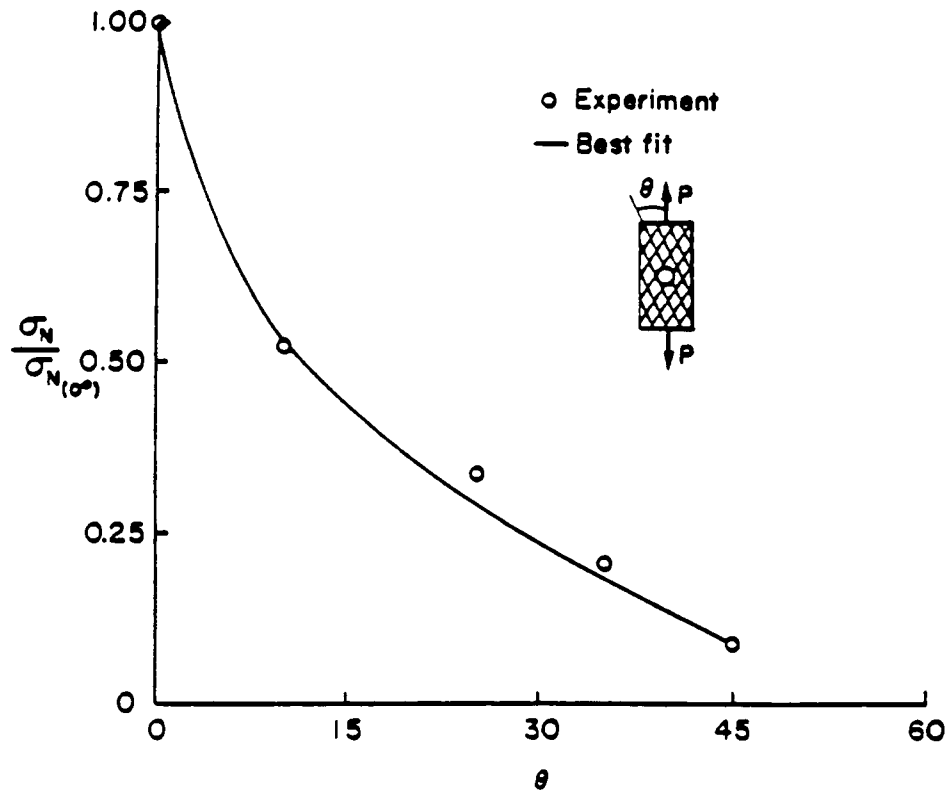

Figure 8. Experimental results obtained for the angle-ply laminates normalized with respect to the notched strength of 0° laminate.

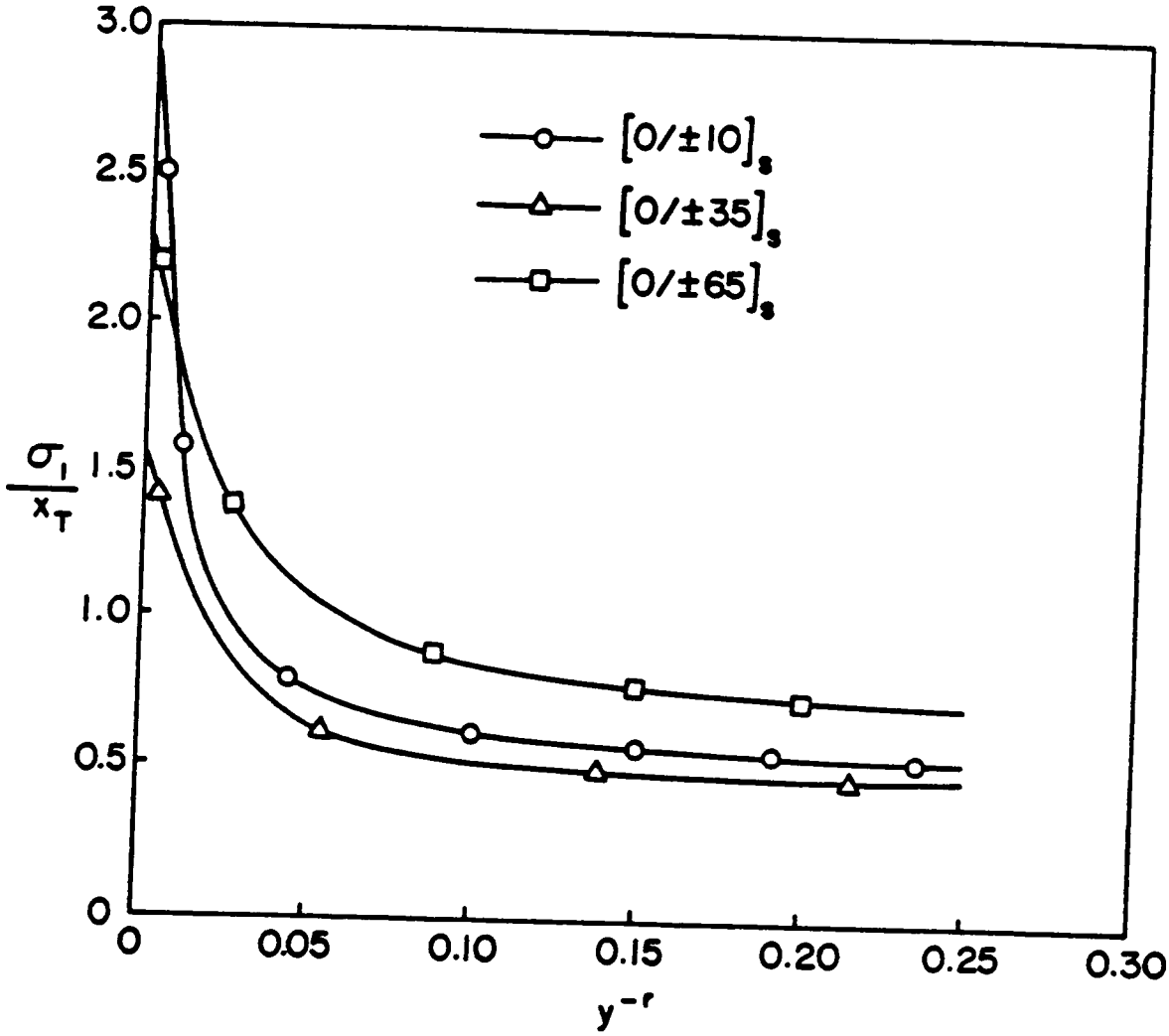

Figure 9. The normalized principal stress versus the distance away from the hole for several $[\,0\,/\,\pm\theta\,]_s$ laminates.

This result encouraged the author to write an invariant equation in terms of D_o and the terms controlling the stress concentration at the boundary of the hole. From Lekhnitskii's solution , the stress at the boundary of the hole is given by

$$\sigma = p[1 + n] \qquad [3.2.2]$$

where p is the applied stress and n is a laminate property that controls the value of the stress concentration. For an orthotropic material n is given by

$$n = \beta + \delta \qquad [3.2.3]$$

where β and δ are the imaginary values of the complex roots μ_1 and μ_2.
The sum $(\beta + \delta)$ determines the stress concentration at the hole and controls the stress distribution away from the hole for the laminate. However, since the failure criterion is based on the ply level, the stress concentration for the controlling ply is needed. Using equations [3.1.1] - [3.1.3], the stress concentration factor for a 0 degree ply can be written as

$$K = \frac{E_1}{E_L}(1 + n)\left[\frac{1 - \nu_{xy}\nu_{21}}{1 - \nu_{12}\nu_{21}}\right] \qquad [3.2.4]$$

where E_L and ν_{xy} are laminate properties in the direction of the zero degree ply. It is important to note that the stress concentration factor defined in equation [3.2.4] is a function of both the material unidirectional properties and the laminate effective engineering properties. For an orthotropic material n can be written in terms of the engineering properties as

$$n = \sqrt{2(\frac{E_L}{E_T} - \nu_{xy}) + \frac{E_L}{G_{xy}}} \qquad [3.2.5]$$

where E_T is the laminate stiffness in a direction perpendicular to the fiber and G_{XT} is the laminate shear modulus.

Equation [3.2.4] was derived for a zero degree ply and $\phi = 0$. In the event that ϕ is different from zero, the stress concentration factor will become a function of ϕ and will occur at a point which is not perpendicular to the direction of the applied load. However it was observed, as will be shown later, that the value of K remains the same but changes position around the circumference for different values of ϕ.

In order to find D_o an invariant equation in terms of the stress concentration factor and the Poisson's ratio is written as

$$\left[\frac{D_O \cdot \nu_{xy}}{K}\right]_1 = \left[\frac{D_O \cdot \nu_{xy}}{K}\right]_2 \qquad [3.2.6]$$

where either D_{o1} or D_{o2} is obtained using experimental data.
The ratios of $\frac{K_2}{K_1}$ and $\frac{\nu_{xy1}}{\nu_{xy2}}$ control the stress distribution at and away from the hole for the 0 degree ply. The results obtained using this procedure are given in table 3, where all the parameters needed are listed. The prediction is started by finding a D_o value from one of the configurations using the experimental notched strength. In table 3, the $[0/\pm 10]_S$ laminate was used to calculate the value of D_o and start the prediction.

As shown in table 3, good agreement between the experimental and predicted data was obtained. It is important to note that for the $[0/\pm 65]_S$ and $[0/90_2]_S$ laminates, the poisson's ratio is less than ν_{12}. For such laminates, the value of D_o needed to reach the applied stress is larger than the rest of the $[0/\pm\theta]_S$ laminates. Therefore, the material unidirectional poisson's ratio was used instead of ν_{xy}.

In order to check this procdure, data given by other investigators were considered. Data given by Whitney and Nuismer [3] were used, and values of D_o were obtained. The strength prediction gave good agreement with their experiments. The results are shown

Table 3.

The notched strength data obtained for $[0/\pm\theta]_S$ laminates. (r = 0.125 in.)

Stacking	K	D_O	ν_{xy}	P_{EX}	P_{PR}
$[0/\pm 10]_S$	6.04	0.075	.532	118.5	118.5
$[0/\pm 25]_S$	5.68	0.034	1.10	78.0	71.0
$[0/\pm 35]_S$	6.24	0.042	1.01	63.0	60.0
$[0/\pm 45]_S$	6.85	0.064	.704	64.0	58.0
$[0/\pm 65]_S$	8.63	0.190	.220	65.0	65.0
$[0/90_2]_S$	14.0	0.308	.032	67.0	69.0

in table 4. Furthermore, data given by Whitney and Kim [13] for $[\pm 45/0/90]_s$ and $[90/0/\pm 45]_s$ laminates were also checked. Again, the predicted results gave good agreement with the experimental data as shown in table 5. It should be noted here that the stress concentration and the poisson's ratio for the two configurations are identical, and hence, the same value of D_o is used. Moreover, table 5 shows the strength for different values of hole diameter, and again the same value of D_o is used, resulting in good predictions. This result leads to the conclusion that, the value of D_o does not depend on the diameter of the hole when used at the ply level.

For more corroboration, data obtained by Lagace [14] were also considered. The strength prediction along with other parameters are shown in table 6. Once again, the good agreement between experimental and predicted data is noted. The ν_{12} value was used to determine the D_o value for the $[0/\pm 75]_s$ and $[0/90_2]_s$ laminates.

Quasi-isotropic laminates loaded at an angle to the material axis:

To further check the capability of the predictive analysis based on the ply level, quasi-isotropic laminates loaded at an angle ϕ with respect to the material axis were examined. The experimental data were obtained by Gurdal [15] at Virginia Tech.

The stress at an angle ϕ was transformed using the laws of transformation to the following

$$\sigma_x = \sigma_\phi \cos^2\phi, \quad \sigma_y = \sigma_\phi \sin^2\phi, \text{ and} \tau_{xy} = \sigma_\phi \sin\phi \cos\phi \qquad [3.2.4]$$

The predicted data were started by finding the value of D_o when ϕ is equal to 0. Once the characteristic dimension was known, the angle was varied and the prediction methodology took place according to the procedure outlined in figure 5. However, because of the presence of shear stresses, the maximum state of stress need not be perpendicular to the laminate x-axis. This is illustrated clearly in figure 10 as given by Lekhnitskii. In

Table 4.

The notched strength predictions using the experimental data obtained by whitney and Nuismer [3].

Graphite/Epoxy

Stacking	K	D_O	ν_{xy}	P_{EX}	P_{PR}
$[0/\pm 45/90]_S$	7.73	0.070	.310	43.0	43.0[x]
$[0/90]_{2S}$	10.6	0.103	.040	55.4	61.0

Glass/Epoxy

Stacking	K	D_O	ν_{xy}	P_{EX}	P_{PR}
$[0/\pm 45/90]_S$	6.10	0.013	.270	27.8	27.8[x]
$[0/90]_{2S}$	6.67	0.015	.090	34.3	30.0

x laminate used to find D_O from experimental data.

Table 5.

The notched strength predictions using the experimental data obtained by Whitney and Kim [13]. ($D_o = 0.105$)

Stacking	R	D_O	ν_{xy}	P_{EX}	P_{PR}
$[\pm 45/0/90]_S$	0.05	0.105	.320	48.8	54.2
$[\pm 45/0/90]_S$	0.15[x]	0.105	.320	40.2	40.2
$[\pm 45/0/90]_S$	0.30	0.105	.320	37.8	33.2
$[90/0/\pm 45]_S$	0.05	0.105	.320	53.3	53.3
$[90/0/\pm 45]_S$	0.15	0.105	.320	43.0	40.3
$[90/0/\pm 45]_S$	0.30	0.105	.320	37.0	33.2

x laminate used to find D_o from experimental data.

Table 6.

The notched strength predictions using the experimental data obtained by Lagace [14]. (r = 0.1197 in.)

Stacking	K	D_O	v_{xy}	P_{EX}	P_{PR}
$[0/\pm 15]_S$	5.58	0.032	.670	85.2	85.2
$[0/\pm 30]_S$	5.78	0.023	1.02	61.6	57.0
$[0/\pm 45]_S$	6.72	0.039	.670	53.2	51.2
$[0/\pm 60]_S$	7.54	0.098	.297	61.8	56.0
$[0/\pm 75]_S$	10.6	0.145	.094	68.0	60.2
$[0/90_2]_S$	13.4	0.184	.033	80.0	62.0

figure 10, an orthotropic plate made out of Birch plywood is loaded at 45° from the laminate x-axis. The distribution of the stress σ_θ is shown and it is clear that the points of maximum stress are not at A and A_1.

For this reason the hole was scanned around the circumference to find the point of maximum stress and apply the failure criterion at that point. Moreover, since the load is applied at an angle, all the plies involved were scanned to insure the application of the failure criterion to the controlling ply. The predicted and experimental data are both shown in table 7. The good agreement between experimental and predicted data should again be emphasized. It was found that for ϕ between 0 and 10, the maximum stress is perpendicular to the laminate x-axis and the 0° ply is the controlling ply. However, as ϕ is varied beyond 10°, the point where the maximum stress occurs is shifted. for example, the maximum stress for $\phi = 15°$ occurs at at an angle of 170° from the y-axis and the controlling ply is still the 0° ply. On the other hand, when ϕ is equal to 22.5°, both the 0° and the 45° ply are oriented at the same angle with respect to the laminate x-axis and both of these plies are supposed to fail simultaneously. Indeed, the prediction shows that both plies fail simultaneously. The failure function versus the angle around the circular hole for both the 0° and 45° plies are shown in figure 11. It should be noted that θ used here denotes the angle around the circumference of the hole. As ϕ is increased beyond 22.5° , the controlling ply becomes the 45° ply and the prediction is based on the failure of this ply. The point of maximum stress for $\phi = 30°$ occurs at an angle of 140° from the y-axis as shown in figure 12. Furthermore, as ϕ reaches 45°, the predicted data should yield similar failure stress as for the case of $\phi = 0°$; and the prediction yielded good agreement.

It should be noted , that the same value of D_o was used to predict the strength of the laminate at different angles. This can be justified by the fact that the same Poisson's ratio and the stress concentration factor, although shifted location, exist.

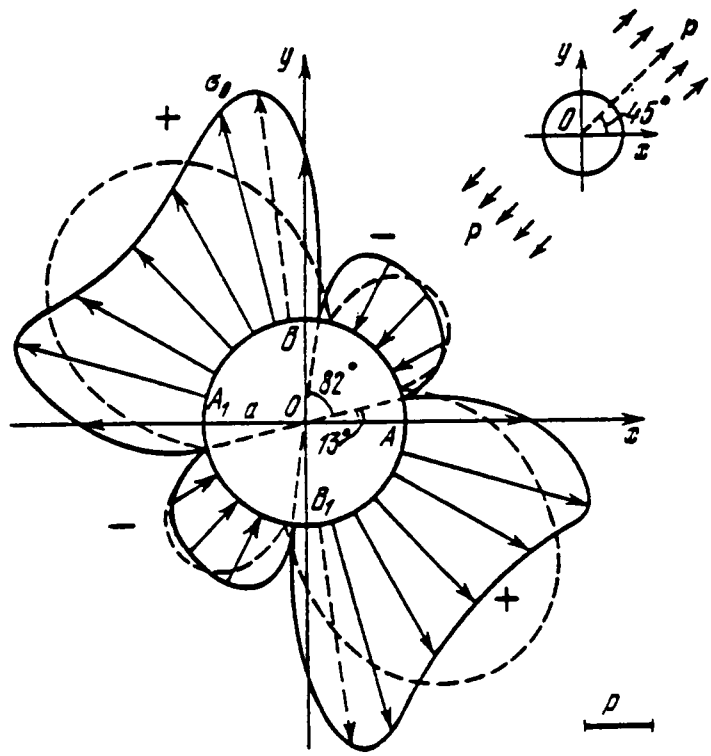

Figure 10. The stress distribution around the hole of a Birch plywood (solid line) loaded at an angle 45 degrees to the laminate x-axis.

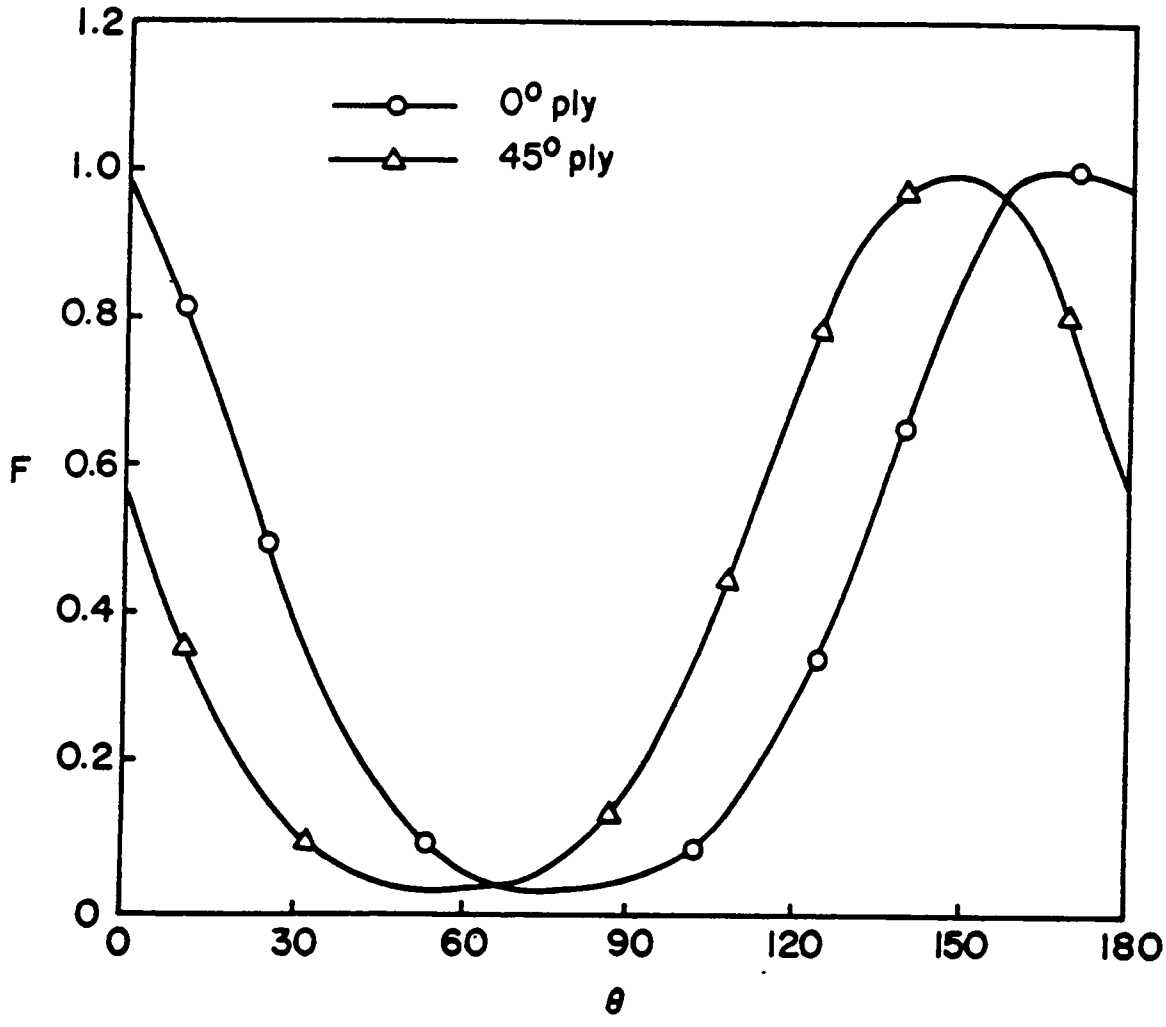

Figure 11. The failure function versus the angle θ around the hole for the quasi-isotropic laminate in the 0 and 45 degree plies.

Table 7.

The prediction of notched strength of quasi-isotropic laminates loaded at an angle ϕ to the material x-axis [15].

ϕ	P_{EX}	P_{PR}	$\beta + \delta$	D_O
0	43.2	42.0	2.0	0.027
5	43.0	43.0	2.0	0.027
10	43.8	44.3	2.0	0.027
15	45.0	45.0	2.0	0.027
22.5	50.0	50.3	2.0	0.027
30	48.0	47.0	2.0	0.027
45	47.2	44.0	2.0	0.027

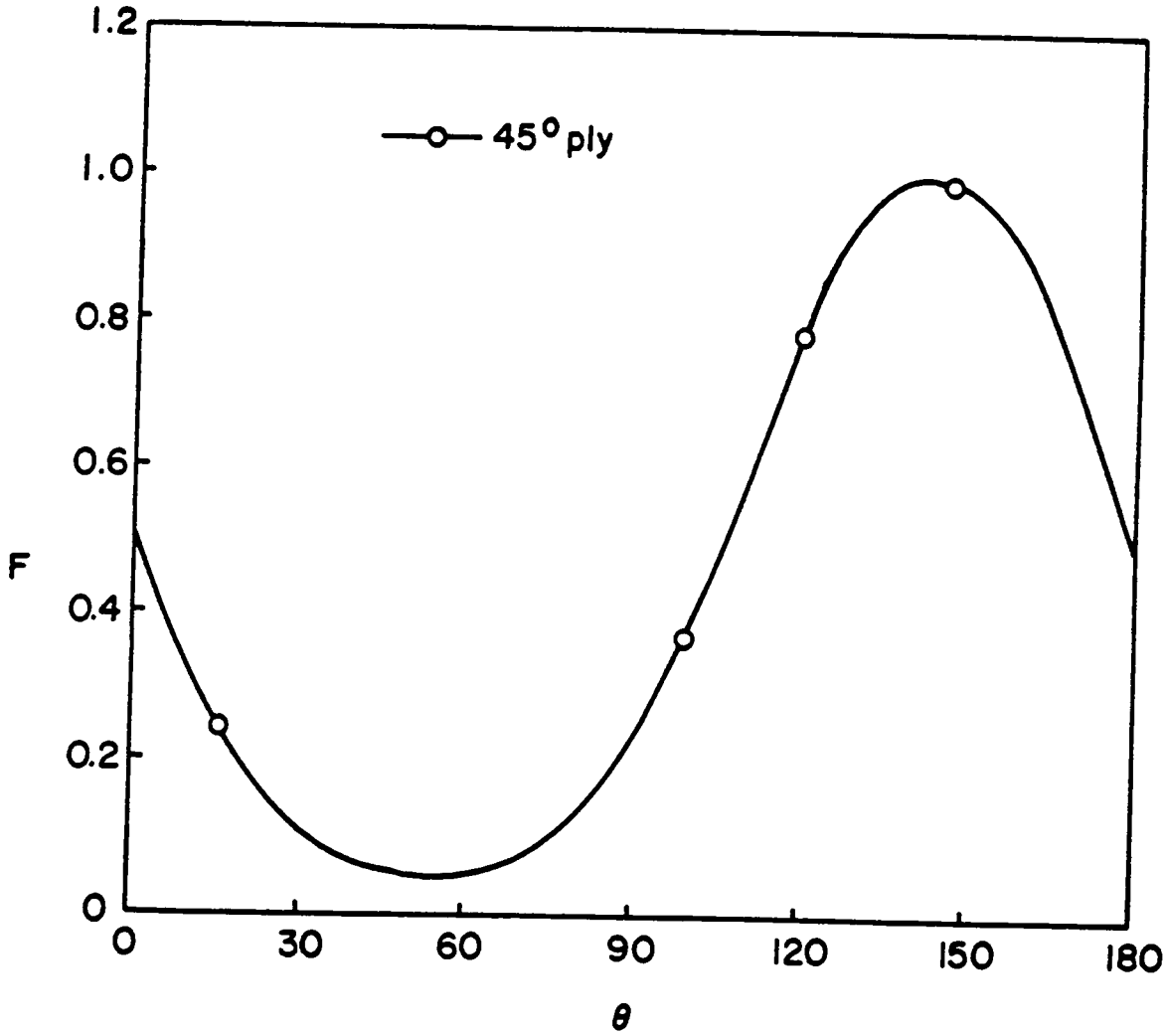

Figure 12. The failure function versus the angle θ around the hole for the quasi-isotropic laminate at $\phi = 30°$.

Chapter IV

Tensile Strength After Impact

The prediction of the tensile strength after impact (TSAI) of composite laminates has not received a great deal of attention by researchers. Few models have been proposed and none are based on practical considerations. In this chapter, the experimental and the prediction of TSAI are treated. The prediction is based on a practical background and involves the measurement of the delaminated area caused by impact damage.

4.1. Material and Specimen Fabrication

The material used in this study is the Hexcel 584/T2L. The unidirectional properties of which were characterized and are shown in table 8. All the specimens used for the impact testing were fabricated at the Composite Materials Fabrication Laboratory at Virginia Tech. The Prepreg was hand laid so as to make the desired stacking sequence. A heavy roller was used to eliminate any air bubble after each lamina was placed. The curing cycle was that recommended by the manufacturer. The panels were cured to achieve 65% fiber volume fraction. The panels were made with 12 X 12 in. dimensions and then cut using a diamond blade to the required specimen size of 6 X 6 in. .

Ultrasonic C-scans were performed on all the specimens to ensure that there was no pre-impact damage present. A typical C-scan is shown in figure 13.

4.2. Experimental Procedure

The experimental program was carried out using a Dynatup Model-8200 drop weight impact test machine. The Model-8200 is appropriate for tests on thin sections of

Table 8.

The unidirectional properties of Hexcel 584/T2L Graphite/Epoxy.

E_1 (MSI)	E_2 (MSI)	ν_{12}	G_{12} (MSI)
18.0	3.25	0.33	0.84

X_T (KSI)	X_C (KSI)	Y_T (KSI)	Y_C (KSI)	S_{12} (KSI)
198	---	25	---	20

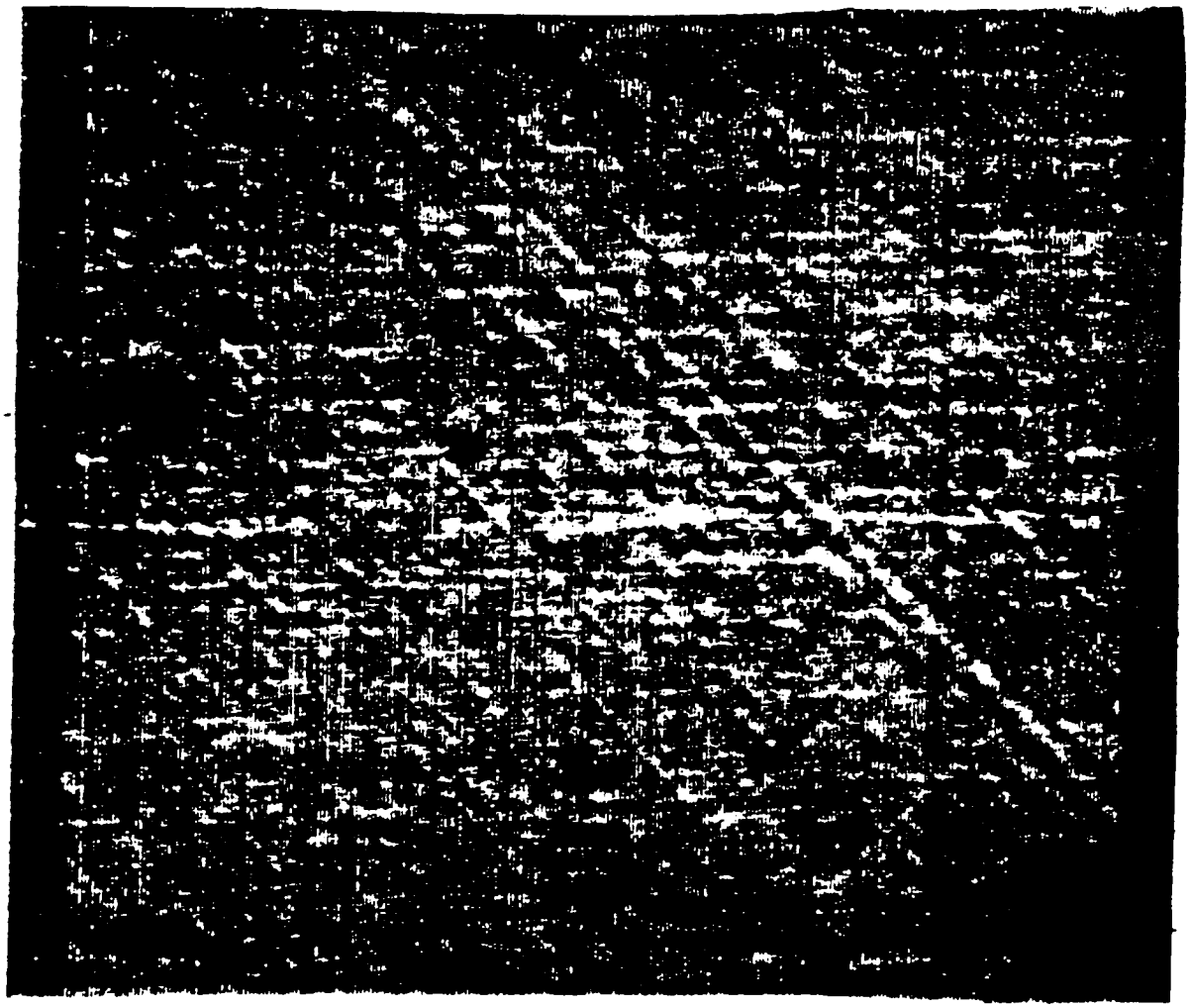

Figure 13. A typical ultrasonic C-Scan of a Hexcel laminate before impact.

brittle plastics, ceramics, and metals. Once the 6 X 6 in. specimen was C-scanned, the specimen was placed in the impact fixture and the tup was dropped from a height depending on the desired impact energy level. A General Research Corporation 730-I data system was used to provide the energy and force versus deflection curves for the impact loading. Typical energy and force versus time curves are shown in figure 14. The specimens were impacted at the center point.

After impact, the specimens were C-scanned to evaluate the delaminated area. The impacted specimens were then cut to 3.5 X 6 in. , making sure that the delaminated area is well within the width of the specimen. As for the tensile test, an MTS machine with hydraulically pressurized grips having a width of 3.75 in. was used. The specimens were loaded to failure and the ultimate load was recorded. The laminate stacking sequences used for this study were $[0/\pm 45/90]_{2s}$ and $[0/\pm 45/0]_{2s}$.

4.3. Predictions and Discussion

The delaminated area resulting from impact damage, is modeled as an elliptic inclusion. The stress analysis for an infinite plate containing an elliptical inclusion was introduced in chapter II. The elastic compliance properties of the inclusion needs to be reduced depending on the amount of impact energy; or more precisely, depending on the delamination resulting from the impact damage.

The approach taken to find the ratio of the compliances of the plate to that of the inclusion, m, defined in equation [2.3.8], is genuine. The factor m is determined under the assumption that some small delaminated area, introduced from a low impact energy, will result in no significant strength loss. This area is measured from the ultrasonic C-scan and used as a reference area. Therefore, to obtain m, the delaminated area at a given impact energy level is scaled to the reference area. This will produce, according to

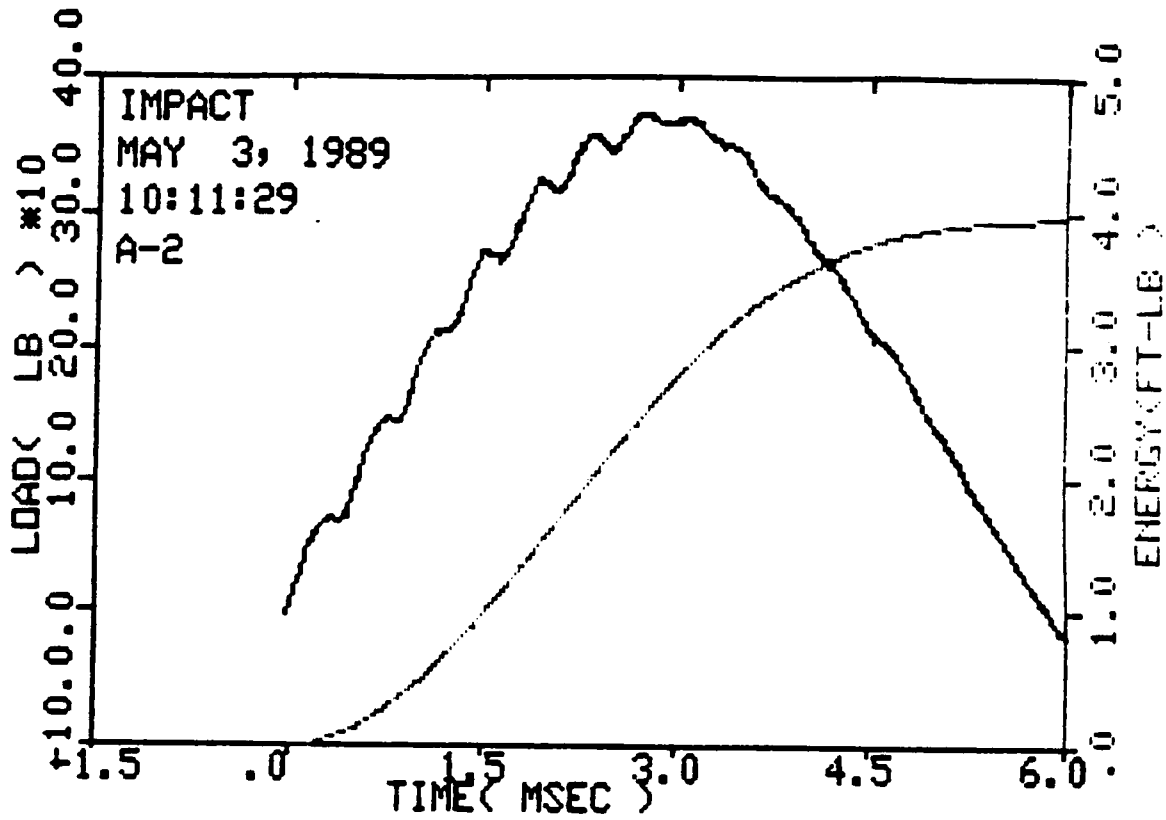

Figure 14. A typical energy and force versus time curves for the impacted specimens.

the assumption, the value of m used in the prediction. Mathematically, this can be written as,

$$m = \frac{A_D}{A_{REF}} \qquad [4.3.1]$$

where A_D is the delaminated area at a specified energy level and A_{REF} is the reference area. In equation [4.3.1], it is assumed that the ratio of the delaminated area to the reference area is proportional to the ratio of the compliances of the plate and the inclusion. That is

$$\frac{A_D}{A_{REF}} = \frac{a'_{ij}}{a_{ij}} = m \qquad [4.3.2]$$

The justification of such an assumption is a hard task. Intuitively, the higher the impact energy, the larger the damage size observed. This observation was the foundation of the model proposed by Caprino [9]. Furthermore, it has been shown that the stiffness degradation is a measure of damage introduced due to mechanical cyclic loading. Stinchcomb and Reifsnider [18] have shown a reduction in the secant modulus of approximately 30%. Observations such as this was also reported by [19].

On the other hand, Kachanov [20] proposed a damage criterion for isotropic materials. The damage criterion is a function of the damaged and the original area of the body. A continuity function was defined by [20], such that

$$\psi = 1 - \frac{A}{A_O} \qquad [4.3.3]$$

where ψ is the continuity function, A is the damaged area, and A_o is the original area. The strength of the material was related to the continuity function by a simple equation

$$\psi = \frac{\sigma}{\sigma_O} \qquad [4.3.4]$$

where σ was defined as the nominal stress and σ_O is the stress related to the original area. By assuming elastic-plastic deformation, the stiffness of the damaged material was related to the continuity function, ψ, as follows

$$E' = \psi \cdot E \qquad [4.3.5]$$

where E' and E are the Young's moduli of the damaged and original material respectively.

Keeping in mind the significance of the continuity function, let us take a look at the existing models proposed to predict the residual strength after impact of composite laminates. The model proposed by Caprino [9] relates the damage strength to the impact energy. It was assumed, as discussed earlier, that a characteristic flaw exist due to a characteristic impact energy level. Below the value of the characteristic impact energy, no reduction in the undamaged strength is expected. Hence, a characteristic flaw size exists below which no reduction in strength is anticipated. Mathematically, the model was written as

$$\frac{\sigma_r}{\sigma_O} = \left(\frac{U_O}{U}\right)^{\alpha} \qquad [4.3.6]$$

where σ_r is the residual strength, σ_O is the undamaged strength, U_O is the characteristic impact energy, U is the impact energy, and α is an experimentally determined parameter. By defining the right hand side of equation [4.3.6] as a continuity function, equation [4.3.6] becomes

$$\frac{\sigma_r}{\sigma_O} = \psi \qquad [4.3.7]$$

therefore, the residual strength can be predicted once the value of the continuity function is determined. Moreover, since Caprino's model assumes that the flaw size can be expressed as a function of the impact energy in terms of a power law, The continuity function, in turn, can be expressed in terms of the damage size in a way similar to that of Kachanov's. It should be noted that the damaged area defined by Kachanov is different than that of Caprino's.

In addition, Husman, et.al., [10] predictive model expresses the residual strength after impact as a function of the impact energy and the energy under the stress-strain curve for statically loaded composites without an implanted hole. The model can be expressed as

$$\frac{\sigma_r}{\sigma_O} = \sqrt{\frac{W_S - K\overline{W}_{KE}}{W_S}} = \psi \qquad [4.3.8]$$

where $\overline{W}_{KE}$ is the impact energy divided by the thickness of the plate and W_S is the energy under the stress-strain curve. Equation [4.3.8] also reduces to finding a continuity function which depends on the impact energy.

Therefore, the assumption made for finding 'm' does have a foundation when compared with other existing fracture and damage models. The value of 'm' is nothing but the continuity function, ψ, defined above.

Once 'm' is evaluated, for every impacted specimen, the stress analysis and the predictive procedure, described in chapters II and III, is carried out here to find the tensile strength after impact.

$[0/\pm 45/90]_{2s}$ and $[0/\pm 45/0]_{2s}$ laminates:

The specimens were cut and impacted at various energy levels resulting in damage that varied from small indentation to complete penetration. The ultrasonic C-scan for the impacted specimen are shown in figures 15 and 16. It should be noted that the term "damage" is used loosely here and does not connote any specific damage phenomenon, such as, fiber breakage or matrix cracking. But, it rather refers to the amount of delamination introduced due to impact.

Figure 15 clearly shows that the damage is not elliptical in shape but varies from one energy level to another. The delaminated area is measured taking into account most of the damage presented, however, the radii of the elliptical inclusion are determined by modeling the damage at the center of the specimen as an ellipse. The experimental and predicted values of the TSAI results, along with the impact energy and the value of m, for the $[0/\pm 45/90]_{2s}$ and $[0/\pm 45/0]_{2s}$ laminates are listed in tables 9 and 10. Tables 9 and 10, show good agreement between the experimental and the predicted data. It should be noted that only one specimen was tested at each impact energy level.

$[(0/90)_4]_s$ laminates:

To check this predictive approach, data obtained by Ghande [16] was used and the strength predictions were obtained. The material used by [16] was T300/934 Graphite/Epoxy. The ultrasonic C-Scans for the impacted specimens are shown in figure 17.

The analysis used for the previous section were repeated here to find the value of 'm' and hence predict the TSAI. The results obtained are listed in table 11. Once again, the agreement between the experimental and the predicted data should be noted.

An important question pertinent to the assumption made to find the factor m need to be raised,i.e does the assumption of a reference area can be retained without a sig-

nificant loss of accuracy ? In table 11, the reference area was obtained at an energy level of 1.8. The prediction at that energy level, where 'm' is equal to unity, yields good agreement with the experimental data. Furthermore, the experimental strength for an undamaged laminate was obtained by [16] to be equal to 127 KSI. A comparison between the undamaged strength and the strength at the reference area shows a reduction of 16%. Even though this data point was obtained from a single test and it is beleived to be too high, the assumptions work well for the predictive scheme as exhibited in tables 9, 10, and 11.

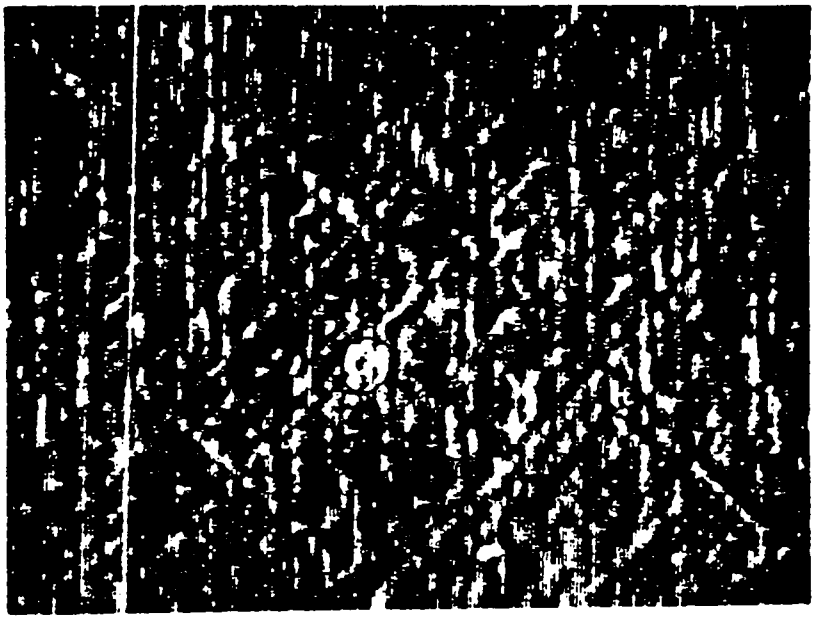

2.3 Ft.Lb.

5.9

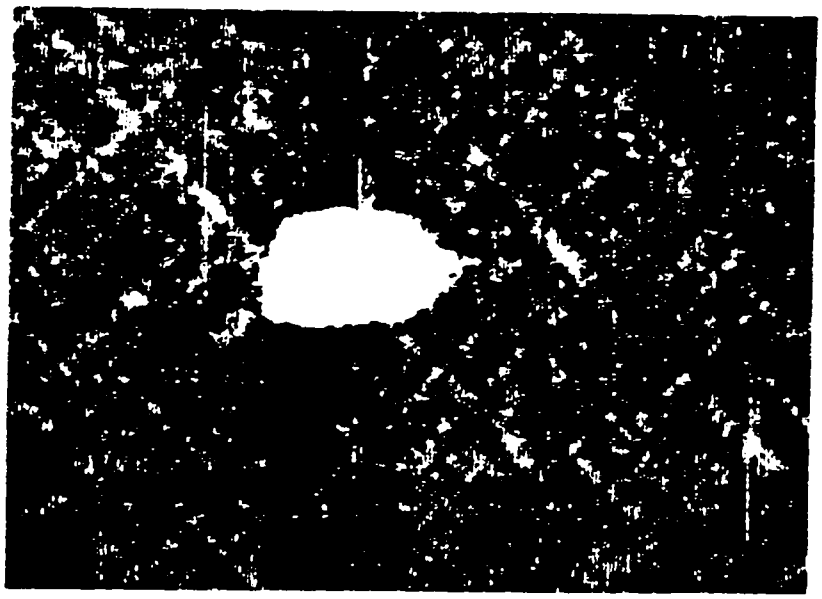

Figure 15. The ultrasonic C-Scan of the $[\ 0/\pm 45/90\ ]_{2s}$ laminates after impact.

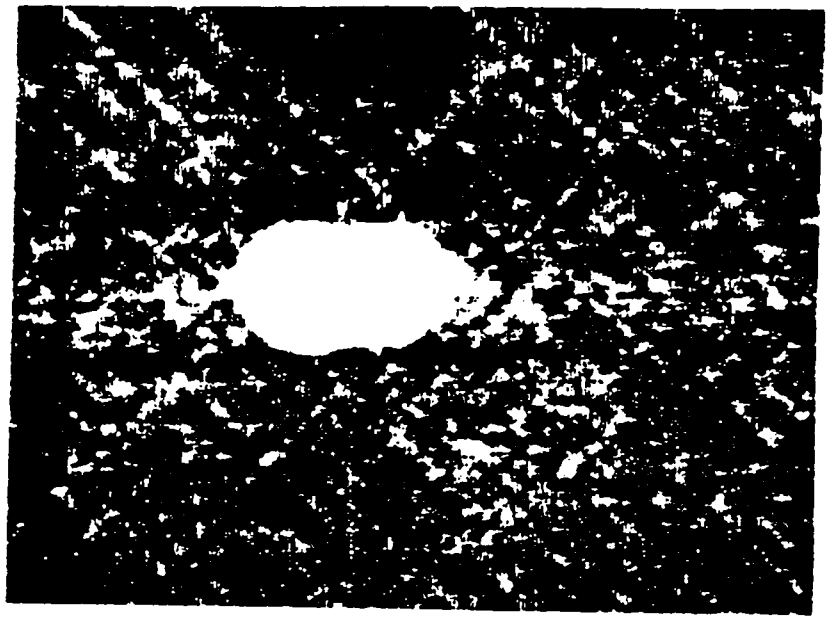

6.6

9.6

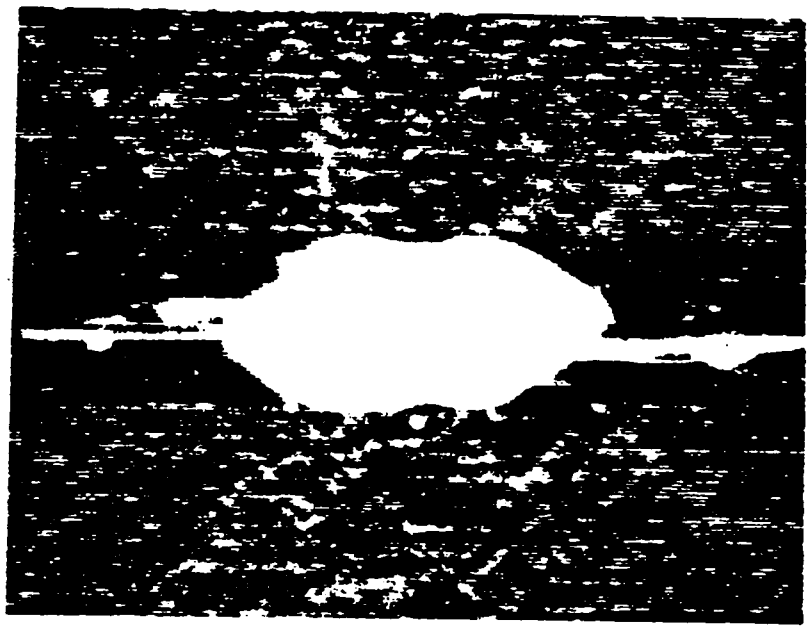

12.5

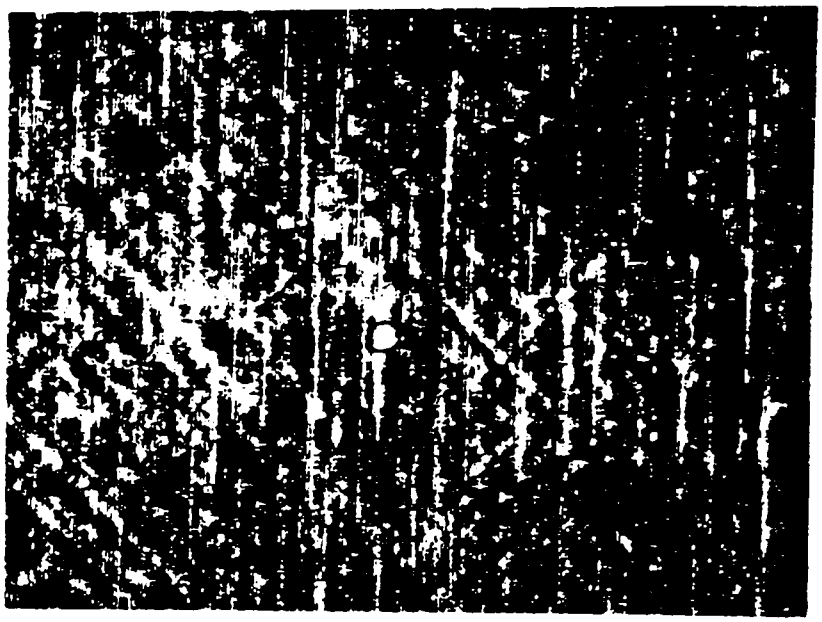

2.3 Ft.Lb.

4.0

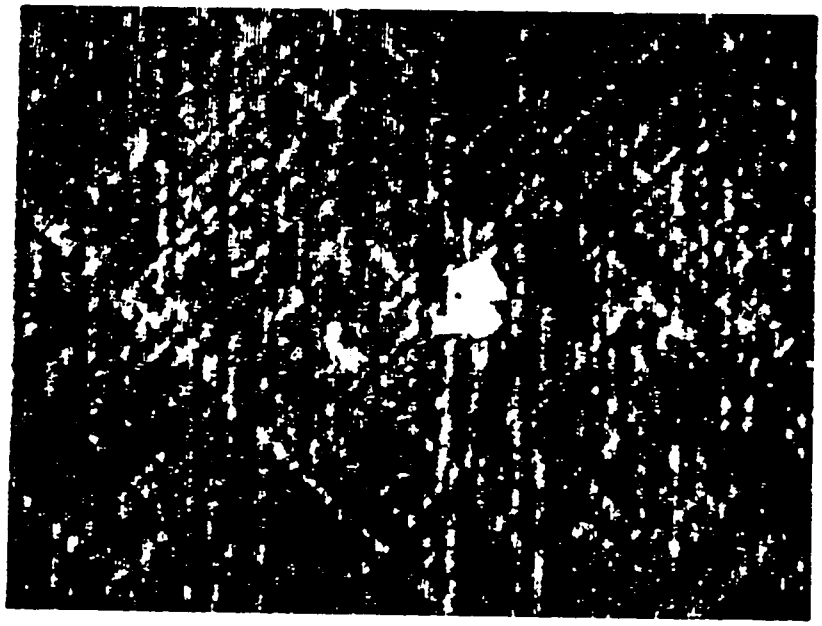

Figure 16. The ultrasonic C-Scan of the $[\ 0\ /\ \pm 45\ /\ 0\ ]_{2\ S}$ laminates after impact.

5.9

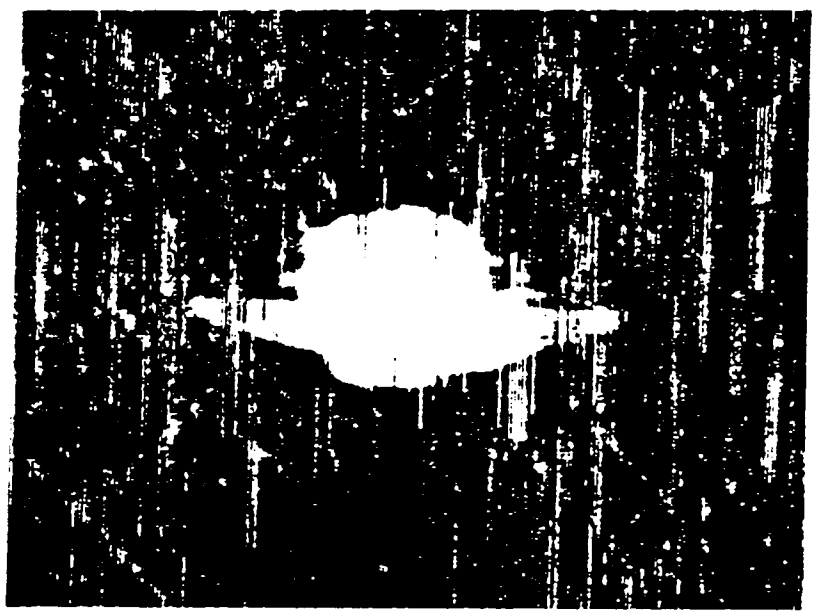

8.9

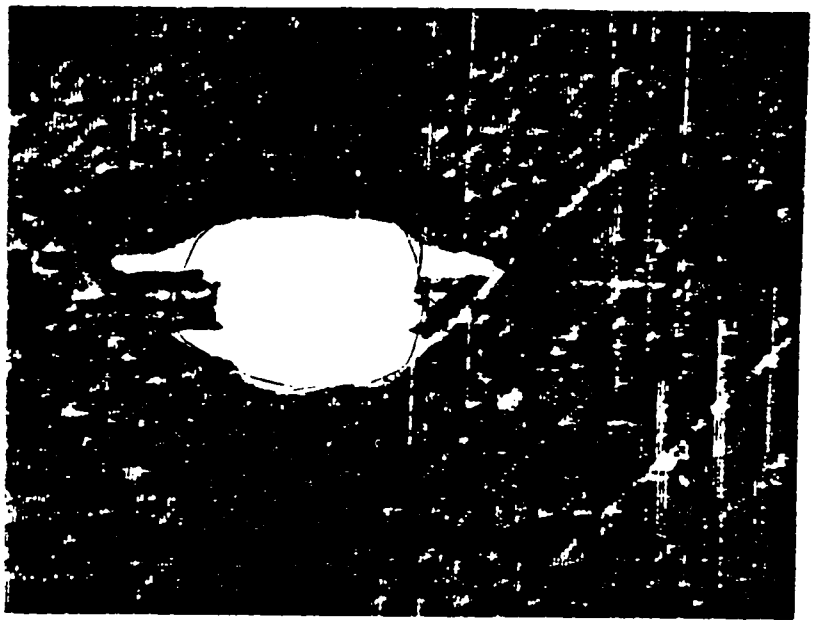

9.7

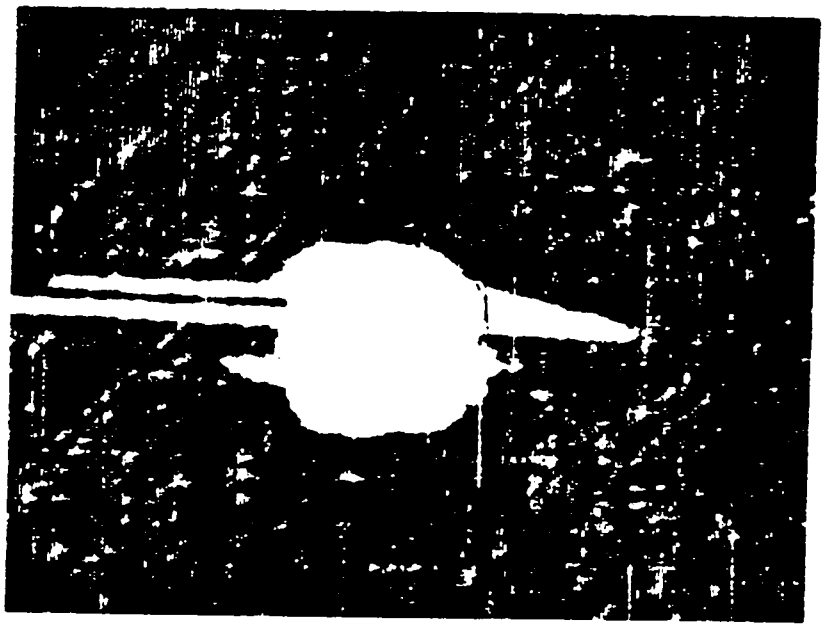

10.3

Table 9.

The tensile strength after impact data for $[0/\pm 45/90]_{2S}$ laminates.

I.E.	A_D	*m*	*A*	*B*	P_{EX}	P_{PR}
2.3	0.02	1.0	0.078	0.078	72.60	85.00
4.0	0.10	5.0	0.156	0.188	72.80	78.00
5.9	0.52	25.9	0.406	0.406	72.10	63.00
8.9	0.74	36.8	0.468	0.500	58.94	60.0
9.7	0.94	47.0	0.438	0.630	55.10	56.40
10.3	0.94	65.0	0.500	0.688	54.40	54.40*

* Laminate used to find D_O .

Table 10.

The tensile strength after impact data for $[0/\pm 45/0]_{2S}$ laminates.

I.E.	A_D	*m*	*A*	*B*	P_{EX}	P_{PR}
2.3	0.05	1.0	0.125	0.125	------	120.0
5.9	0.49	9.8	0.312	0.500	112.3	105.0
6.6	0.68	13.6	0.334	0.630	111.7	100.0
9.6	0.98	19.6	0.312	0.750	108.1	97.0
12.5	2.10	42.0	0.470	1.250	84.20	84.20[x]

x Laminate used to find D_o .

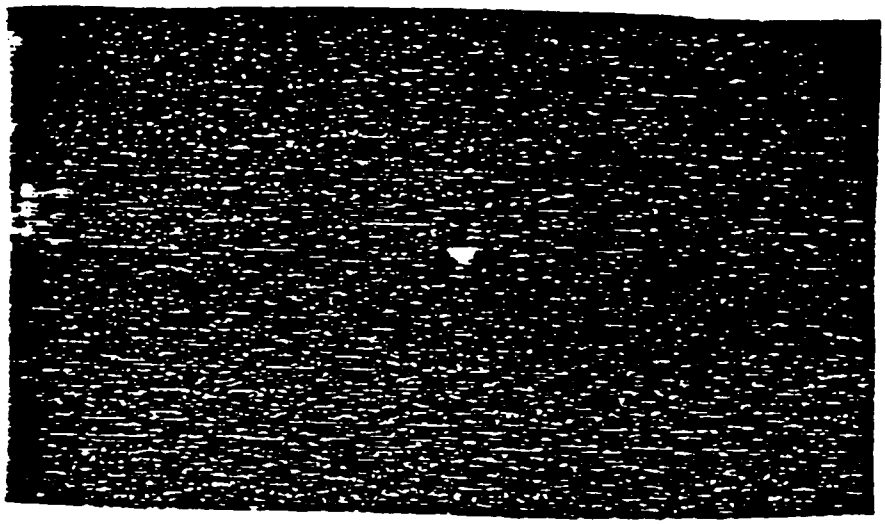

1.7 Ft.Lb.

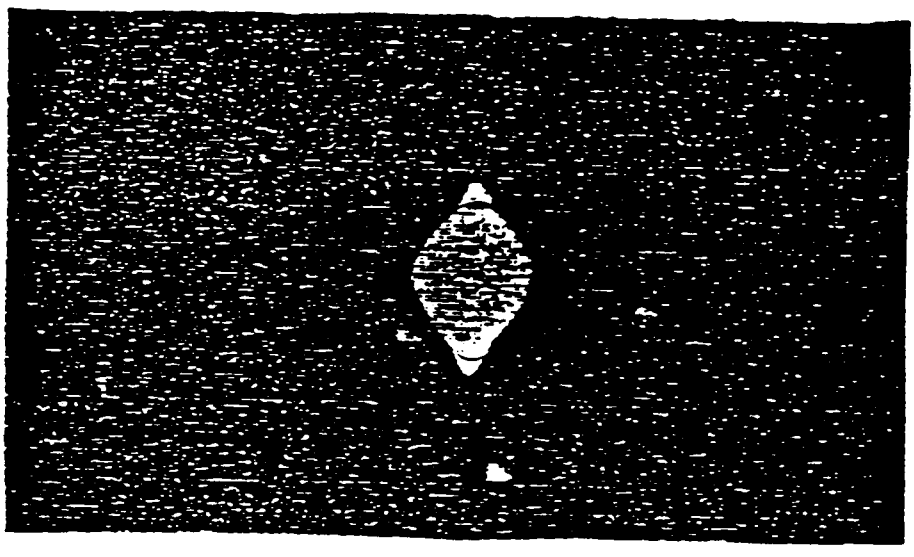

2.4

Figure 17. The ultrasonic C-Scans for the T300/934 impacted specimens.

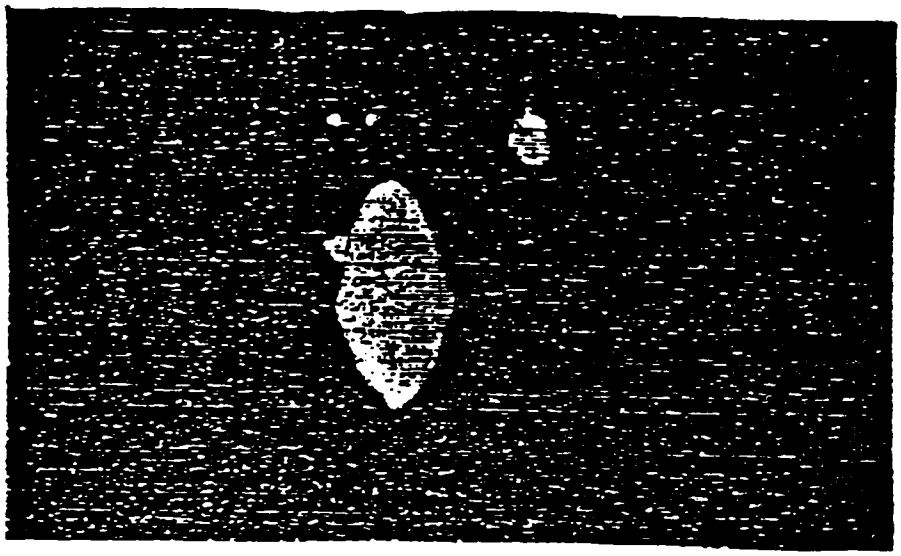

3.4

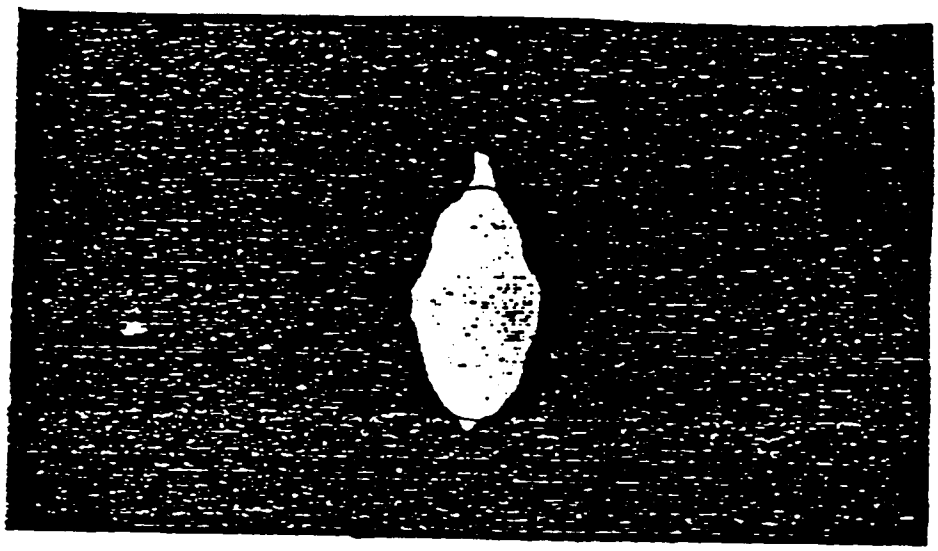

4.0

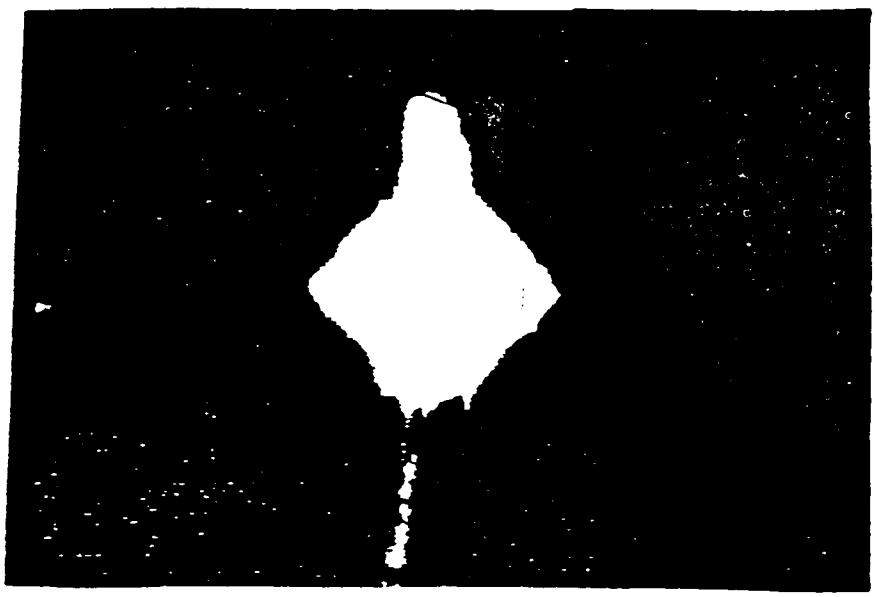

10.3

Table 11.

The tensile strength after impact data for T300/934 laminates [16].

$[(0/90)_4]_S$

I.E.	A_D	*m*	*A*	*B*	P_{EX}	P_{PR}
1.8	0.02	1.0	0.050	0.050	105.0	102.0
2.4	0.35	17.5	0.300	0.400	76.00	67.00
3.4	0.48	24.0	0.300	0.550	65.00	61.00
4.0	0.58	28.5	0.350	0.600	53.00	58.0
10.3	1.05	52.5	0.450	0.800	50.00	50.00*

* Laminate used to find D_o .

Chapter V

Conclusions and future Work

The tensile strength of notched and impact damaged laminates was investigated. The advantages gained using the proposed model to predict the notched strength are listed below:

1. The unnotched strength of a laminate is not required.

2. The value of D_o remains the same for laminates with different hole sizes.

3. The D_o value for any laminate of a given material system can be evaluated from one experiment. For laminates with other configurations the invariant equation obtained is used to evaluate D_o .

4. The same value of D_o can be used for laminates loaded at different angles to the material axis.

The conclusions of the results acquired can be summarized in the following:

1. The notched strength of the $[0/\pm\theta]_s$ laminates can be predicted based on the average stress criterion applied to the controlling ply.

2. The value of the characteristic dimension D_o can be determined using an invariant equation based on the laminate Poisson's ratio and the stress concentration factor of the controlling ply.

3. The strength of laminates loaded at an angle to the material x-axis can be predicted by scanning the hole in the controlling ply, for the point of maximum stress and applying the failure criterion starting at that point.

4. The notched strength of off-axis unidirectional laminates can be predicted using a matrix-based failure criterion applied at a critical point on the boundary of the hole. This is equivalent to a point stress criterion, where the characteristic dimension is equal to zero.

5. The notched strength of angle-ply laminates could not be predicted due to the different failure modes existing among the different $[\pm\theta]_s$ laminates. An interesting phenomenon was observed in the $[\pm 45]_s$ laminate, where the maximum principal stress is not maximum at the hole boundary; but the maximum occurs at a distance away from the hole. This makes the use of the average stress criterion based on the ply level a little complicated; if used, care should be taken to account for the position of the maximum stress.

6. The tensile strength after impact can be obtained by simulating the damage caused by impact as an elliptical inclusion. A reference area is defined where a very small amount of damage was introduced. The ratio of the delaminated area to that of the reference area is assumed to be proportional to the ratio of the compliances of the plate and the inclusion, m.

The formulation presented before can be the foundation for many future investigations, some of which are:

1. To study the validity of the invariant equation used to find D_o for different stacking sequences and laminates that are not fiber dominated.

2. To use the modelling of impact damage to predict the compressive strength after impact, which is becoming a crucial test in damage tolerence analysis.

3. To provide a more rigorous basis for the invariant used to determine D_o .

4. To determine the generality of the present analysis.

Bibliography

1. Waddoups, M. E. , Eisenmann, J. R. , and Kaminski, B. E. , Journal of Composite Materials, Vol. 5, pp. 446-454 (1971).

2. Wu, E. M., "fracture Mechanics of Anisotropic Plates," in Composite Material Workshop, S. W. Tsai, J. C. Halpin, and N. J. Pagano, pp. 20-43 (1968).

3. Nuismer, R. J. and Whitney, J. M., "Uniaxial Failure of Composite Laminates Containing Stress Concentrations," in Fracture Mechanics of Composites, ASTM STP 593, pp. 117-142 (1975).

4. Poe, C. C., Jr. and Sova, J. A., "Fracture Toughness of Boron/ Aluminum Laminates with Various Proportions of 0° and $\pm 45^{\circ}$ Plies," NASA Technical Paper 1707 (November 1980).

5. Mar, J. W. and Lin, K. Y., "Fracture Mechanics Correlation for Tensile Failure of filamentary Composites with Holes," Journal of Aircraft, Vol. 14, No. 7, pp. 703-704 (1977).

6. Karlak, R. F., "Hole Effects in a Related Series of Symmetrical Laminates," in Proceedings of Failure Modes in Composites, IV., The Metallurgical Society of AIME, Chicago, pp. 105-117 (1977).

7. Pipes, R. B., Wetherhold, R.C. and Gillespie, J. W., Jr. ," Notched Strength of Composite Materials," J. of Composite Materials, Vol. 13, pp. 148-160 (1979).

8. Jonathon Awerbuch and Madhu Madhukar ," Notched Strength of Composite laminates: prediction and experiments - A review," J. of Reinforced Plastics and Composites, Vol. 4, pp. 3 , (1985).

9. G. Caprino, " Residual Strength Prediction of Impacted CFRP Laminates ," J. of Composite Materials, Vol. 18, (1984).

10. G. E. Husman, J. M. Whitney, and J. C. Halpin, " Residual Strength Characterization of Laminated Composites Subjected to Impact Loading," ASTM STP 568, PP. 92-113, (1975).

11. V. Sarma Avva and H. L. Padmanabha,"Compressive Residual Strength Prediction in Fiber-Reinforced Laminated Composites Subjected to Impact Loads," ICF, Advances in Fracture Mechanics, Vol. 4, (1984).

12. S. G. Lekhnitskii, Anisotropic Plates, Gordon and Breach Science Publishers, (1968).

13. Carol A. Ginty and Christos C. Chamis,"Fracture Characteristics of Angle-Plied Laminates Fabricated from Overaged Graphite/Epoxy Prepreg," ASTM STP 948, PP. 101-130, (1987).

14. J. M. Whitney and R. Y. Kim,"Effect of Stacking Sequence on the Notch Strength of Laminated Composites," ASTM STP 617, PP. 229-242, (1977).

15. Paul A. Lagace,"Notch Sensitivity and Stacking Sequence of Laminated Composites," ASTM STP 893, PP. 161-176, (1986).

16. Z. Gurdal, ESM Department, Virginia Tech, unpublished data.

17. Gajanan V. Ghande, "Impact Response of Interleaved Composite Materials," M.S. thesis Virginia Tech, Dec.(1986).

18. W. W. Stinchcomb and K. L. Reifsnider, "Cumulative Damage Model for Advanced Composite Laminates," Virginia Tech, CCMS-86-05, 1986.

19. C. E. Bakis and W. W. Stinchcomb, "Fatigue Response of Notched Laminates Subjected to Cyclic Loads," Virginia Tech, CCMS-86-04, 1986.

20. L. M. Kachanov, Introduction to Continuum Damage Mechanics, Martinus Nijhoff Publishers, 1986.

The vita has been removed from the scanned document